ENHANCEMENT OF BIOLOGICAL ACTIVITY IN BIOFILTERS BY AMINO ACID SUPPLEMENTATION

by

Bofu Li

Submitted in partial fulfilment of the requirements for

the degree of Master of Applied Science

at

Dalhousie University
Halifax, Nova Scotia
August 2016

DEDICATION

For my parents and Shijun.

TABLE OF CONTENTS

LIST OF TABLES

LIST OF FIGURES

ABSTRACT

Biological filtration has been gradually accepted by water utilities for supplying economic and high quality drinking water. To achieve optimal growth during biological filtration a balance of available carbon (substrate) and nutrients such as nitrogen and phosphorus should be available for biological growth. The literature has suggested a carbon (C): nitrogen (N): phosphorus (P) ratio of 100:10:1 for successful growth. To achieve this balance, previous studies have added inorganic nutrients (nitrogen and phosphorus) as chemical amendment for biofiltration. However, results with inorganic nitrogen and phosphorus have been mixed and many studies have not seen improvement through the addition of these chemical agents. This thesis addresses this gap in the literature by examining the role of organic nitrogen as chemical amendment to enhance biological growth in a reproducible manner. Amino acids were used as the source of organic nitrogen as previous work has demonstrated that amino acids are biologically available in drinking water systems. Thus the hypothesis of this work is that of amino acids amendment can enhance biological filtration by increasing active biomass. In this study, the specific growth rate was increased from 0.058 h^{-1} to 0.094-0.148 h^{-1} in filtered flocculated water with addition of amino acids. The biomass adenosine triphosphate (ATP) of the estimated growth model was increased from 220-640 pg/cm^2 to 3.2×10^4-2.9×10^5 pg/cm^2 in amino acid supplemented biofilters with the target concentration of 3 mg amino acid/L. The areal biodegradation rate (k_a) of amino acids was found to be in the range of 0.0015-0.1196 m/h.

LIST OF ABBREVIATIONS USED

µg	Microgram
AAs	Amino Acids
Acetyl-CoA	Acetyl Coenzyme A
AOC	Assimilable Organic Carbon
AR	Annular Reactor
ATP	Adenosine Triphosphate
Avg.	Average
BDOC	Biodegradable Dissolved Organic Carbon
B. subtilis	Bacillus Subtilis
BOM	Biodegradable Organic Matter
C	Carbon
℃	Celsius Degree
CFU	Colony Forming Units
cm^2	Square Centimeter
COD	Chemical Oxygen Demand
COD_{Cr}	Dichromate COD method
COD_{Mn}	Permanganate Index
Con.	Concentration
DBPs	Disinfectant By-Products
DGGE	Denaturing Gradient Gel Electrophoresis
DO	Dissolved Oxygen

DOC	Dissolved Organic Carbon
DOM	Dissolved Organic Matter
E. Coli	Escherichia Coli
EBCT	Empty Bed Contact Time
EPS	Extracellular Polymeric Substance
ESI	Electrospray Ionisation
FEEM	Fluorescence Emission Excitation Matrix
FAD	Flavin Adenine Dinucleotide
$FADH_2$	Flavin Adenine Dinucleotide (Reduced)
GAC	Granular Activated Carbon
GDP	Guanosine Diphosphate
GTP	Guanosine Triphosphate
h	Hour
HPC	Heterotrophic Plate Count
HPLC	High Pressure Liquid Chromatography
HRT	Hydraulic Retention Time
JDKWSP	J. D. Kline Water Supply Plant
KH_2PO_4	Potassium-Biphosphate
L	Liter
LC-MS	Liquid Chromatography – Mass Spectroscopy
m^3	Cubic Meter
mg	Milligram
mg/L	Milligram Per Liter

min	Minutes
ML	Million Liters
mL	Milliliter
m/z	Mass Over Charge Ratio
N	Nitrogen
NAD	Nicotinamide Adenine Dinucleotide
NADH	Nicotinamide Adenine Dinucleotide (Reduced)
NH_4Cl	Ammonium Chloride
NOCs	Nitrogenous Organic Compounds
NOMs	Natural Organic Matters
OUR	Oxygen Uptake Rate
P	Phosphorus
peCOD	Photoelectrochemical Oxygen Demand
PES	Polyethersulfone
pg	Picogram
pH	Potential Hydrogen
PO_4-P	Phosphate
ppm	Parts Per Million
PARAFAC	Parallel Factor Analysis
P. fluorescens	Pseudomonas Fluorescens
psi	Pounds Per Square Inch
rRNA	Ribosomal Ribonucleic Acid
SUVA	Specific Ultraviolet Absorbance

T	Time
ThOD	Theoretical Oxygen Demand
TiO_2	Titanium Dioxide
TOC	Total Organic Carbon
V	Volt

ACKNOWLEDGEMENTS

I would like to thank my supervisor Dr. Graham Gagnon for giving me the opportunity and confidence to pursue graduate studies in Canada. This work would not be possible without his extensive knowledge and great supports.

I also gratefully acknowledge and extend thanks for the financial support provided through the NSERC/Halifax Water Industrial Research Chair program. Additionally, this work was funded by NSERC STEWARD Program scholarship. As well, I would like to thank Shujie Fu, Dr. Yuri Park, Amina Stoddart, Benjamin Trueman, Jordan Schmidt, Lindsay Anderson, Yamuna Vadasarukkai, Sean MacIssac, Brett Penney, Lauren Fleet and Heather Daurie for their help with the analysis and technical support at the Dalhousie University.

Chapter 1 Introduction

1.1 Impetus for work

Drinking water treatment technologies provide various ways to treat different qualities of raw water from various water sources. Among these technologies, conventional filtration has economic advantages in the production of high-quality drinking water. In general, biological filtration (biofiltration) has been adapted from conventional filtration to achieve removal of both particles and biodegradable organic compounds due to lacking of inhibition (e.g., chlorine) in raw water and the accumulated biomass on filter media (Urfer et al., 1997). The advantages of biofiltration include the ability to remove disinfection by-product (DBP) precursors (Sketchell et al., 1995, Wang et al., 1995, Chaiket et al., 2002) and organic micropollutants (Zearley and Summers, 2012) and the ability to supply biologically-stable water to distribution systems (Urfer et al., 1997). Biological filtration has been gradually accepted by more and more water treatment utilities as an alternative system to conventional rapid sand filtration (Lauderdale, 2011).

The biological activity of biofilm is an important indicator for assessing the operational performance of biofilters. Wang et al. (1995) indicated that better removal of natural organic matter (NOM) and DBP precursors may be correlated with higher biomass in the biofilter, especially with the biological activity of biomass. In order to achieve higher biological activity in biofilters, nutrient and substrate supplements for biofilters are possible ways to change the passive treatment process to the purposefully enhanced treatment process (Lauderdale et al., 2012). Increased removal of organic compounds and biological activity caused by phosphate supplementation have been observed in many

previous studies (Miettinen et al., 1997; Yu et al., 2003; Lauderdale et al., 2011, 2012). These previous studies focused on inorganic nutrients (e.g., phosphate) and hydrocarbons (e.g., acetic acid and ethanol). Lauderdale (2011) pointed out that carbon addition alone would exacerbate the nutrients limitation in biofilters. Additionally, hydrocarbons addition may have negative impacts on removal of secondary substrate and terminal headloss. Even though suggested empirical molecular formulas for bacterial growth are different in literature (Metcalf and Eddy, 2003; Rittmann and McCarty, 2001), carbon:nitrogen:phosphorus ratio (C:N:P) is regarded as an important indicator of bacterial growth. Keeping a reasonable C:N:P ratio is of importance to keep good operational performance of biological treatment. Therefore, comprehensive supplementation, which can diminish nutrient limitation, is a better way to enhance biological activity of biofilm in biofilters.

van der Kooij and Hijnen (1988) reported the growth of *Aeromonas hydrophila* in drinking water with a cocktail containing 21 amino acids. The average half velocity constant was 8.0 μg C/L, which is equal to the concentration of the rate-limiting substrate at the one-half maximum specific growth rate. Bacteria demonstrate a great affinity for amino acids because of the active transport (Anraku, 1978). Gagnon and Huck (2001) also reported high biodegradability of three amino acids (aspartic acid, glutamatic acid, and serine) in biofilm reactors.

According to related published studies on drinking water (Miettinen et al., 1997, van der Kooij and Hijnen, 1988), drinking water biofilms (van der Kooij et al., 1995; Gagnon and

Huck, 2001), and enhanced biofilters (Yu et al., 2003; Lauderdale et al.,2012; Granger et al., 2014), enhancement with amino acids could improve the treatment efficiency of biofilters.

1.2 Thesis hypothesis

The hypothesis for this thesis is that the addition of amino acids in biofilters results in a significant promotion of biological activity and leads to a higher treatment efficiency of natural organic matter.

Based on the literature review the basis for this hypothesis are:

- amino acids are able to provide carbon and nitrogen for the biosynthesis of protein and nucleic acid, which can solve the nutrients limitation of biofilm;
- amino acids can be rapidly utilized by biofilm on filter media through active transportation within empty bed contact time (EBCT) because of their relative small molecular size;
- amino acids (phenylalanine, tyrosine, and tryptophan) have a high energetic cost that contribute to biosynthesis in proteomes. Consequently, through utilizing amino acids bacteria can reduce energy cost for multiplication and achieve higher growth rates and biological activity through critical acid cycle and oxidative phosphorylation.

1.3 Thesis objectives and outline

This thesis investigates the related kinetics and the changes in biological activity of biofilm by dosing amino acids (phenylalanine, tyrosine, and tryptophan). The experiments used three distinct approaches: i) A batch experiment to investigate the changes in biomass adenosine triphosphate (ATP) in filtered flocculated-water with dosing amino acids and nutrients (i.e., nitrogen and phosphate); ii) Bench-scale biofilters to examine the relationship between the biological activity of biofilm grown on filter media and amino acid degradation; and iii) Bench-scale biofilm reactors to investigate the kinetics of biofilm growth and amino acid degradation.

Chapter 1- Provides the thesis objective, the outline, and the impetus for this thesis, and introduces a possible way to enhance biofilters.

Chapter 2- Provides a brief history of biological filtration and nutrient supplementation for biofilters. This chapter also introduces the theory and application of the analysis methods used in this study: ATP measurement, photoelectrochemical oxygen demand (peCOD) measurement, and fluorescence emission excitation matrix (FEEM) generation. The background of the catabolism of amino acids in bacteria is also introduced.

Chapter 3- Examines the feasibility of improving biomass ATP in filtered floc-water from J.D. Kline Water Supply Plant. A batch experiment is used to investigate the ATP increase and total organic carbon (TOC) removal with five days incubation period.

Chapter 4- After testing the feasibility of enhancing biomass ATP in surface water, four bench-scale biofilters were used to investigate the changes in biomass ATP, degradation of amino acids, and removal of natural organic matter (NOM). This experiment included a long-term enhancement process and a mathematic model of biomass ATP growth. The degradation of organic compounds was measured by dissolved organic carbon (DOC) and peCOD, and fluorescence spectroscopy.

Chapter 5- To investigate the relationship between the biological activity of biofilm and amino acid concentrations, ATP measurement and liquid chromatography–mass spectroscopy (LC-MS) were applied to measure biomass ATP and degradation of amino acids in three biofilm reactors.

Chapter 6- The results of the three experimental chapters are summarized. Recommendations for further studies are also given.

Chapter 2 Background and Literature Review

2.1 Biological filtration

2.1.1 Filtration and biological filtration

Modern water treatment technologies provide various choices for treating raw water at any given water source. However, the economic factor is still one of critical limitations in the selection of water treatment processes rather than technical issues. Compared with other energy-intensive water treatment technologies (e.g., reverse osmosis), the "conventional" filtration has its advantages to supply economic high-quality drinking water (Huisman and Wood, 1974).

Filtration is regarded as a way of water treatment which dates back from 1804 when John Gibb, the owner of a bleachery, and others who designed and installed the slow sand filter system in Paisley, Scotland (Huisman and Wood, 1974). In 1829, filtration was adopted by an engineer James Simpson, as a way of water treatment for public supply by constructing an installation to treat the water from Chelsea Water Company in London (Huisman and Wood, 1974). In 1872, the first public successful application of filtration was in Poughkeepsie, New York, USA (Logsdon et al., 2006).

Filtration removes particles and some of pathogenic bacteria by porous and granular filter media. According to different functions, filtration can be categorized into slow sand filtration, high rate filtration, and biological filtration.

Slow sand filtration is the first effective municipal water treatment system (Lauderdale, 2001), but it is not widely used in drinking water industry now. In addition to filtration function, slow sand filtration also uses biological treatment to remove the nutrients and organic compounds in raw water with the indigenous microorganism grown on filter media. Nevertheless, slow sand filtration facilities require a large area of land and low loading rates (U.S. EPA, 1990). It also needs low turbidity of influent and high maintenance efforts to clean and replace filter media. Therefore, slow sand filtration cannot meet the requirement of urban development and increased population.

High rate filtration has a better performance on the flexibility of raw water quality (Conley, 1972) and requires less area of land than conventional slow sand filtration. High rate sand filtration is the most common system to remove particles in drinking water treatment. Due to the advantages of high rate sand filtration, most drinking water treatment plants in North America have switched their water treatment systems from slow sand filtration to high rate filtration (Lauderdale, 2011). High rate filtration focuses on the removal of suspended particles, but the appearance of microorganisms on filter media is unavoidable with long running time. With the widespread use of chlorine (Bellar et al, 1974) and other disinfectants in disinfection process, the biological treatment caused by accumulated microorganism is inhibited by backwash water (Miltner et al., 199 5) and chlorinated influent. This suppressive function of disinfectants reduces the biological activity of microorganism in filters. Nowadays, these suppressive-biological high rate filtration systems are widely used across North America (Lauderdale, 2011).

Biological filtration was developed to remove suspended particles, nutrients, and biodegradable organic compounds. Unlike slow sand filtration and high rate filtration, biological filtration can satisfy the land requirement and water demand in modern cities without dosing inhibitor in influent (e.g., pre-chlorine). Recently, drinking water treatment utilities realize that biological filtration is becoming an alternative system (Lauderdale, 2011). The reason for this interest in biological filtration include: (i) biological filtration is being regarded as a green technology in water treatment industry (Lauderdale, 2011); (ii) The new regulatory of drinking water guideline pushes utilities to look for an water treatment system to reduce the formation of disinfectant by-products (DBPs) and other contaminants; (iii) biological filtration can supply the biologically-stable water to avoid negative impacts in distribution system (Urfer et al., 1997); (iv) The emergence of ozone application in biofilters can improve the biodegradation capability of influent to avoid the taste, odor, and aesthetic problems (Nerenberg et al., 2000; Srinivasan and Sorial et al., 2011).

2.1.2 Nutrient supplementation

Nutrient limitation of biofilters can be assessed by the C:N:P ratio (Basu et al., 2015). Microbial cells consist of various proteins, fats, carbonates and nucleic acids. Species of elements in microorganism are more than four major elements (i.e., carbon, hydrogen, oxygen, and nitrogen). Phosphate, sulfate, iron, and other elements usually are trace elements in bacteria (Rittmann and McCarty, 2001). The molecular formulas of heterotrophic microorganisms are various in water treatment systems. The empirical molecular formula of microbial cells in previous studies are also different. Rittmann and

McCarty (2001) summarized empirical molecular formulas for different substrates and environment conditions. Metcalf and Eddy (2002) suggested that empirical molecular formula is $C_{55}H_{77}O_{22}N_{11}P$ which can avoid the nutrient-limited condition. The generalized C:N:P molar ratio is 100:10:1 which is accepted in aerobic drinking water treatment to optimize the microbial growth (LeChevallier et al., 1991).

In general, organic carbon acts as a growth-limiting substrate in drinking water treatment. Assimilable organic carbon (AOC) is defined as a portion of organic carbon which can be utilized by microorganisms for growth. van der Kooij et al. (1982) investigated the relationship between the growth of *P. fluorescens* strain P17 colonies and AOC concentration in drinking water. AOC usually constitutes 0.1 to 0.9% of DOC in raw water and treated water (van der Kooij et al., 1982). AOC is strongly correlated with the regrowth of heterotrophic bacteria when AOC concentration is higher than 10 µg acetate-C/L (van der Kooij et al., 1982; 1992). In previous studies, AOC has a strong association with bacterial growth (van der Kooij et al., 1992; LeChevallier et al, 1993) in the Unites States and many regions in the Europe where natural water with high mineral nutrients (Miettinen et al., 1997).

In addition to AOC, phosphorus is regarded as an important indicator for regrowth of microorganisms in drinking water distribution system. Phosphorus can improve the bacterial growth in boreal regions, like Finland, where the content of AOC is not obviously correlated with bacterial growth (Miettinen et al., 1997). Miettinen et al. (1997) investigated the heterotrophic plate count (HPC) for surface water, artificial recharge

groundwater, and groundwater in Finland. This study indicated that bacterial growth is correlated with the available phosphorus in the range of 1-50 µg/L PO_4-P. Sathasivan and Ohgaki (1997; 1999) investigated the nutrient limitation in Tokyo's metropolitan drinking water distribution system. They confirmed the phosphorus is the limiting nutrient instead of other inorganic nutrients.

Yu et al. (2003) conducted a phosphorus supplementation study on two pilot-scale granular activated carbon (GAC)-sand dual media biofilters in China. The bacterial growth measured by HPC increased was up to 54 % in the phosphorus-supplemented biofilter. Permanganate index (COD_{Mn}) removal in phosphorus-supplemented biofilter increased from average 15 to 20.56% while the control one was 14.54%. Sang et al. (2003) investigated organic carbon removal in bio-ceramic filters with phosphorus addition. At 25 µg/L PO_4-P (C: P ratio was 100:1.6), the biomass measured by phospholipid increased by 13-22% and oxygen uptake rate (OUR) increased by 35-45% at different filter bed depths. The TOC removal in phosphorus-supplemented biofilter was in the range of 22.0-26.6%. The TOC removal in the control biofilters was in the range of 17.1-21.3%. Biodegradable dissolved organic carbon (BDOC) removal in phosphorus-supplemented biofilter was about 15 % higher than control one. Lauderdale et al. (2012) maintained C:N:P ratio of 100:10:1 on a molar basis in biofilters by dosing phosphate. The headloss decreased by more than 15 % in the nutrient-enhanced biofilter which was corresponded to the decreased extracellular polymeric substance (EPS). Nutrient- enhanced biofilter removed 75% DOC, and ATP increase by 30%. Granger et al. (2014) investigated manganese removal with 20/200 µg/L phosphate in bench-scale granular activated carbon (GAC)/anthracite direct

biofilters. The phosphorus amendment does not affect the manganese removal. However, the average removal of DOC was 23% in the enhanced column which was 11% higher than the control column. With additional phosphorus, biomass ATP attached by GAC and anthracite increased by 97% and 20%, respectively.

Li et al. (2010) used 16S rRNA genes to evaluate the microbial community in both bench-scale and pilot-scale biological active carbon reactors with phosphorus addition. The results of clone library demonstrated that microbial community in two reactors had totally different responds even though two reactors achieved the same performance of contaminant removal.

2.2 Biological activity and organic carbon removal in biofitlers

Biomass ATP is regarded as an important indicator for biological activity in biofilters. In recent years, ATP analysis has been widely used in drinking water treatment to quantify the biomass in treatment systems and distribution systems (Evans et al., 2013; Magic-Knezev and van der Kooij, 2004; Delahaye et al., 2003). Pharand et al. (2014) reviewed the published data of ATP analysis and organic carbon removal in drinking water biofilters. However, the relationship between biomass ATP and organic carbon removal is still unclear due to the limited number of studies.

Velten et al. (2007) investigated the biomass development in drinking water GAC filters using ATP analysis. The start-up phase of the biomass was characterized by a decrease in DOC removal efficiency and an increase in ATP concentration on the GAC particles. In

addition, Velten et al. (2011) used the same method to investigate the characterization of GAC biofilters at different filter bed depths. The biomass accumulated rapidly at all depths within three-month star-up period. The transitions from the start-up period to the steady state period followed a paradigm shift in the biofilter performance. Organic carbon removal decreased as the biomass increased in biofilter because of the adsorption saturation of GAC (Velten et al. 2007).

Biological activity is considered as a possible reason for the organic matter removal, rather than the amount of biomass. Wang et al. (1995) and Segar and Rothman (1996) indicated a possible association between biomass ATP and organic matters removal. These studies also pointed out that the biological activity might be the primary reason for organic matters removal. Wang et al. (1995) observed a trend between biomass concentration and removal of NOM and DBP precursors in anthracite biofilters during start-up phase. The NOM and DBP precursor removals were consistent as the biomass concentration measured by phospholipids gradually increased during day 70 to day 190. Therefore, organic matter removal was likely correlated with biological activity which may be affected by temperature, water quality, backwashing and type of substrate (Wang et al., 1995). Segar and Rothman (1996) reported the increase in biological activity which was caused by more easily biodegradable organic matters after ozonation. Naidu et al. (2013) reported AOC and DOC removals were 90% and 59%, respectively, at high ATP concentration (5.10± 11.8 μg ATP/g media) in seawater-fed biofilters. This demonstrated a relationship between biomass ATP and organic matters removal.

Boon et al. (2011) used 16S rRNA gene-DGGE and ATP analysis to investigate the bacterial community and dynamics in a GAC biofilter. As the amount of biomass in all different sections achieved at the steady-state phase (day 90-160), the average biomass ATP were 10cm=1.2×10^6 g ATP/g GAC, 45cm=1.8×10^6 g ATP/g GAC, 80cm=1.2×10^6 g ATP/g GAC, and 115cm=10.8×10^6 g ATP/g GAC. DOC removal increased along the four sections of the GAC biofilter. The significance of the gene pool demonstrated that community structure parameters (i.e., richness, dynamics, and evenness) are the important parameters determining high functionality of GAC biofilter. Yachi and Loreau (1999) pointed out that high richness and dynamics could build an ecosystem to guarantee the system's operation and protect from the declines in functionality.

2.3 Water quality analysis

2.3.1 Biomass measurement

Numerous analysis methods are available to estimate the biological activity of biofilm. This research project focuses on the application of adenosine triphosphate (ATP) to quantify the active biomass in biofilters.

As the energy carrier in cellular metabolism, ATP is the primary compound for most biochemical enzymatic reactions (Tifft and Spiegel, 1976). ATP could be found in some very rare non-biological conditions, such as the solution of adenine and ribose under ultraviolet irradiation (Ponnamperuma et al. 1963). However, ATP is still commonly regarded as a critical indicator for living creatures and biochemical systems.

The relationship between ATP and conventional biological activity analysis methods have been investigated in some previous studies. HPC is regarded as a traditional parameter to evaluate the microorganisms in drinking water distribution systems and biofilm reactors (Yu et al., 2003; Huck and Gagnon, 2004). Delahaye et al. (2003) conducted an investigation on the relationship between log (ATP) and log (HPC) in Paris's drinking water distribution system where 50% of drinking water originates from surface water and other 50% comes from groundwater. The result demonstrates that there is a linear relationship between log (ATP) and log (HPC) in drinking water distribution. Findlay et al. (1989) used phospholipids technique to measure microbial biomass content in sediments. Then this method was adapted by Wang et al. (1995) for the biomass of biofilters. Dewdell (2012) indicated that the correlation coefficient was 0.91 between biomass ATP and phospholipids content without outliers.

2.3.2 Quantifying natural organic matter by photoelectron-chemical oxygen demand (PeCOD)

Chemical oxygen demand (COD) is an important parameter to assess the effect of organic pollution in water (Balconi et al., 1992; Barker et al., 1999). peCOD is a rapid and environmentally friendly analysis method for determing the COD in water using photoelectrocatalytic oxidation and electric field. It requires less time to complete an assay without a harmful reagent compared with the conventional COD method (Stoddart and Gagnon, 2014).

Hoffmann et al. (1995) summarized the environmental application of semiconductor photocatalysis. TiO_2 is the dominant photocatalyst in photoelectrocatalytic oxidation. Organic compounds can be mineralized on the surface of TiO_2 nanopacticles under UV illumination as shown in Figure 2.1. Illumination of TiO_2 with a photon would result in the promotion of an electron between valence band (VB) and conduction band (CB) by the great energy (i.e., E_g = 3.2eV). This results in photoholes in the valence band with a powerful oxidation capacity for almost all organic matters in water (Qiu et al., 2012).

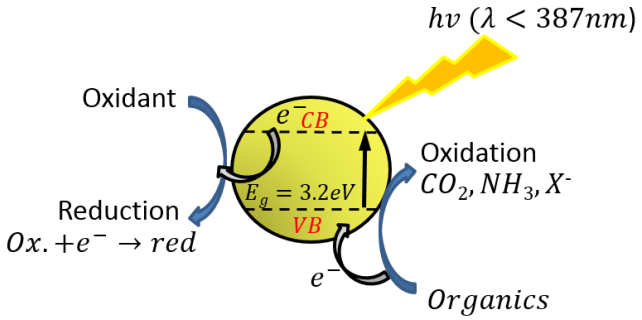

Figure 2.1 Photocatalytic oxidation and reduction processes at TiO_2 nanopaticle.

The reaction rate of organic matters depends on how fast the photoelectrons at conduction band and photoholes are utilized. This is the rate limiting step of overall mineralization process (Equation 2.1). As to traditional TiO_2 photocatalysis system, the photoelectron, which plays as the electron acceptor, was accepted by oxygen. Therefore, COD concentration can be calculated by the decreased dissolved oxygen in water with a sensitive oxygen probe (Qiu et al., 2012). However, oxygen is a weak reducing reagent and low dissolve oxygen in aqueous solution (e.g., less than 10 ppm at 25℃, 1 atm). This is the major drawback of traditional TiO_2 photocatalysis system. Using permanganate (Zhu et al., 2006) and ceriumions (Chai et al., 2006; Song et al., 2009) as the electron acceptors is a

possible solution. In addition, transferring the photoelectron to the external circuit is a better option to solve this problem.

$$C_xH_yO_zX_q + \left(x + \frac{y-2z-q}{4}\right)O_2 \rightarrow xCO_2 + xH^+ + qX^- + \left(\frac{y-x}{2}\right)H_2O \qquad \text{Equation 2.1}$$

TiO_2 can be immobilized on different materials including polymer compounds, titanium, or stainless steel. (Kavan et al., 1996; Liu et al., 1997; Yu et al., 2003). The immobilized nanostructured TiO_2 on conducting materials works as the working electron. The electric field creates a force to separate photoelectron from TiO_2 particles (Zhang et al., 2004) (shown in Figure 2.2) which can improve oxidation efficiency. Therefore, the combination of working electron and electric field make oxidation process easier for transferring the photoelectron to the auxiliary electrode through the external circuit (Zhang et al., 2004). Thus, the reduction reaction takes place on the auxiliary electrode instead of adsorbed O_2 (Qiu et al., 2012).

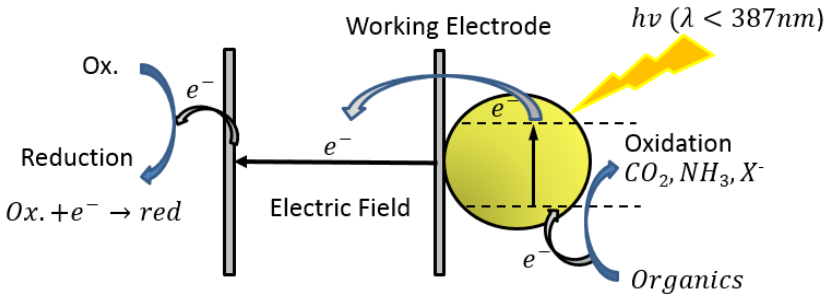

Figure 2.2 Schematic of photoelecrocatalytic processes with TiO_2 thin film electrode.

Zhang et al., (2004) suggested the general equation for mineralization at TiO_2 photoanode (Equation 2.2). Then, the amount of electron transferred at the TiO_2 nanoporous film electrode can be quantified and converted to COD concentration Farady's Law. (Zhang et al., 2004).

$$C_yH_mO_jN_kX_q + (2y-j)H_2 \rightarrow yCO_2 + qX^- + kNH_3 + (4y-2j+m-3k)H^+ + (4y-2j+m-3k-q)e^- \quad \text{Equation 2.2}$$

Kim et al. (2001) described a titanium dioxide (TiO_2) photocatalytic sensor for the determination of COD with the flow injection analysis system. This study demonstrated a linear relationship with COD_{Mn} for treated wastewater in the range of 0.12-8 ppm (Kim et al., 2001). The maximum current was correlated with the flow rate and the amount of TiO_2 beads. Zhang et al. (2004) used a TiO_2 nanoparticle film electrode as the working electrode to promote the degradation efficiency. The detection limitation was 0.2 ppm and the linear range of peCOD was 0 to 360 ppm for industrial wastewater in Queensland State, Australia. In order to completely oxidize the nitrogenous organic compounds (NOCs), Li et al. (2012) used hydroxyl organic compound (i.e., glucose) to improve oxidization capability. The first application of peCOD in drinking water for NOMs was described by Stoddart and Gagnon (2014). peCOD is correlated with theoretical oxygen demand (ThOD) in drinking water.

2.3.3 Characterization and quantification of natural organic matter by fluorescence-spectroscopy

The organic molecules of water samples would be excited by absorbing an emitted photon in fluorometer. Then organic molecules drop in vibrational levels of ground electronic state by emitting photon (Guilbault et al., 1990). A three dimensional fluorescence matrix is generated through an emission map. This matrix can be used to evaluate relative abundance or concentration of organic compound in relevant excitation/emission regions.

In general, fluorescence instruments consist of a source of light, a sample holder, excitation/emission monochromaters (or filters), and a detector as shown in Figure 2.3.

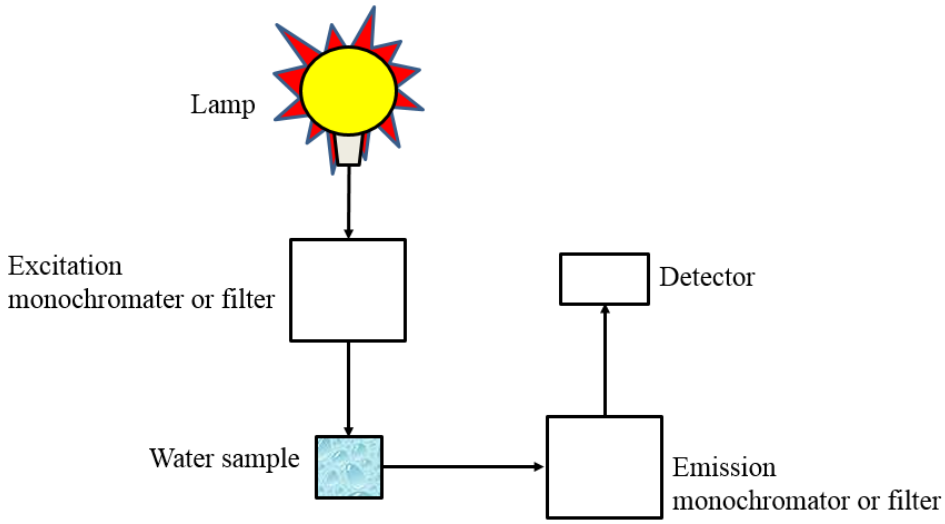

Figure 2.3 Typical components of a fluorescence spectrometer.

Various fluorescence spectroscopy techniques are widely used in detection of organic matters in water. Vodacek et al. (1995) proved that the dissolved organic matter (DOM) is correlated with DOC. Baker (2002) investigated the impacts of wastewater from tissue mill

using fluorescence spectroscopy. The high concentration tryptophan and fluorescent whitening agents in wastewater resulted in a significant fluorescence characteristic of river water. Chen et al. (2003) investigated the organic matters in surface water with and without wastewater pollution. Five major categories of organic matters were shown in different excitation/emission regions using the fluorescence regional integration (FRI) method. Carstea et al. (2010) used florescence spectroscopy to monitor the organic matters in the river. The intensity of humic-like and protein-like peaks increased with a rainfall or a diesel pollution.

2.4 Amino acids in metabolism

Amino acids can be utilized and broken down by the bacteria through different metabolic and catabolic pathways. Barker (1981) reviewed the amino acid degradation in anaerobic bacteria. Teufel et al. (2010) reported the detail catabolic pathways of phenylalanine in bacteria. Christensen et al. (1999) investigated the catabolism of phenylalanine, tyrosine, and tryptophan in lactic acid bacteria. From the perspective of energy cost, Akashi et al. (2002) calculated the metabolic efficiency and amino acid composition in the proteomes of *E.coli* and *B. subtilis* using synonymous codon usage bias.

The metabolism and the catabolism of amino acids are usually related with critic acid cycle (shown in Figure 2.4) and oxidative phosphorylation. As to the oxidation of amino acids, the amino group bonded to the alpha carbon next to the carboxylate terminus is removed during the deamination process (Rittmann and McCarty, 2001). The equation (Equation 2.3) is as below:

$$R - CHNH_2COOH + NAD^+ + H_2O = R - COCOOH + NH_3 + NADH + H^+ \quad \text{Equation 2.3}$$

In general, amino acids convert to acetyl coenzyme A (acetyl CoA), and then enter critic acid cycle. Some of amino acids convert into other amino acids such as succinate, fumarate, and oxaloacetate. These amino acids can directly enter the critic acid cycle to release the energy (Rittmann and McCarty, 2001). Critic acid cycle is the critical part of catabolism of amino acids. The general steps of critic acid cycle are shown in Figure 2.4. Acetyl CoA firstly combines with the oxaloacetic acid and water to form citric acid. For oxidation of Acetyl CoA, the net result of all the reactions is showed in Equation 2.4.

$$CH_3COSCoA + 3NAD^+ + FAD + GDP + Pi + 3H_2 \rightarrow 2CO_2 + 3NADH + FADH_2 + GTP + 3H^+ + HSCoA \quad \text{Equation 2.4}$$

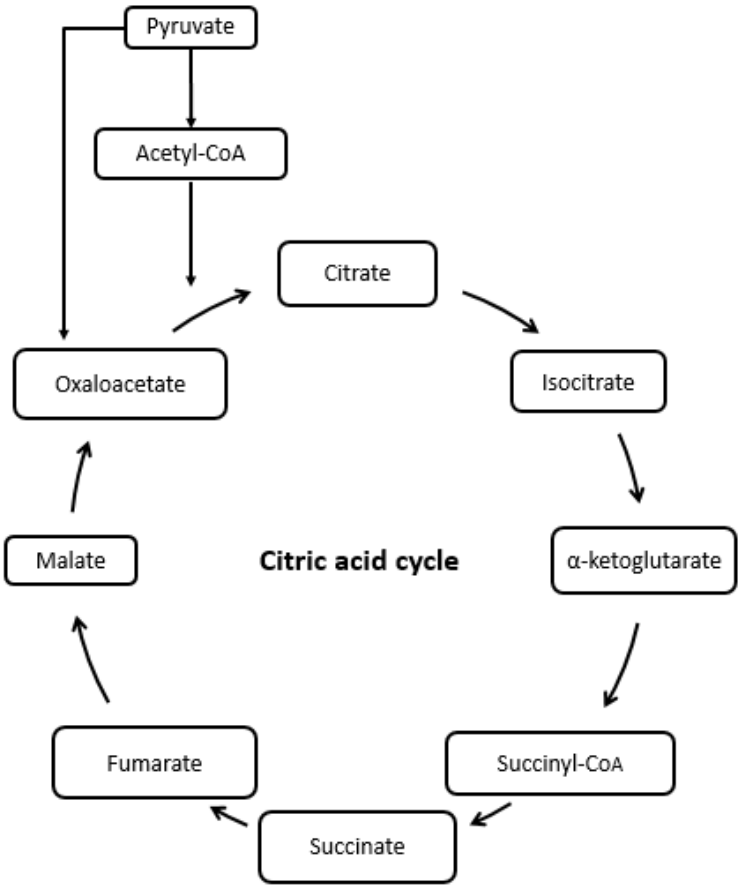

Figure 2.4 Overview of the citric acid cycle.

After the deamination and the critic acid cycle, the energy stored in NADH and $FADH_2$ are converted into ATP to maintain the metabolism processes in bacteria through oxidative phosphorylation. Oxidative phosphorylation can transfer the potential energy to ATP through two major functions: transferring the electrons from NADH to the terminal electron acceptor by a cascade of membrane-bound protein and cytochromes; the protons are released and transferred to the outside of the cell membrane or accumulated OH^+ inside of the cell membrane when the electron transfers from NADH to the terminal acceptor (Rittmann and McCarty, 2001). In this study, the terminal acceptor could be the oxygen in water. The amino acids used in this study are shown in Table 2.1.

Table 2.1 Molecular structure, chemical formula, and ThOD of amino acids (adapted from Pitter and Chudoba, 1990).

Amino acids	Molecular structure	Chemical formula	Molecular weight	ThOD/Mass g/g
L-Alanine	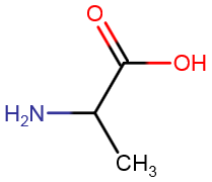	$C_3H_7NO_2$	89.09	1.08
L-Phenylalanine	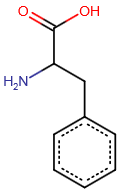	$C_9H_{11}NO_2$	165.08	1.94
L-Tyrosine	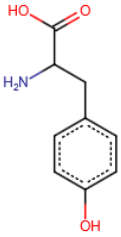	$C_9H_{11}NO_3$	181.07	1.68
L-Tryptophan	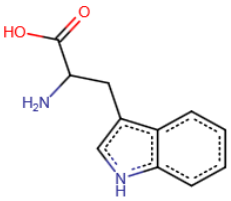	$C_{11}H_{12}N_2O_2$	204.09	2.06

As to drinking water treatment, Dotson and Westerhoff (2009) investigated 16 full-scale drinking water treatment plants in the United States. The average free amino acids in raw water was 0.38 µg/L. In addition, Gagnon and Huck (2001) showed that amino acids were

degraded rapidly by drinking water biofilms. Thus, in the natural environment amino acids are rarely present as free substrate as they are readily degraded by biomass

2.5 Summary of literature review

In conclusion, biological filtration is becoming more popular in the drinking water treatment industry. Biological activity is an important indicator for biofilters. Therefore, both nutrients and substrate amendments are possible ways to change a passive biological treatment to a purposeful biological treatment. As to analysis instruments, ATP, peCOD, and fluorescence spectroscopy are used to assess the operation of biofilters. The amino acid supplementation may improve the biological activity of biofilm in biofilters.

Chapter 3 Amino Acid Batch Experiment

3.1 Introduction

Previous studies demonstrated that mineral nutrients (e.g., phosphate) and substrate supplement may increase biological activity in water. van der Kooij and Hijnen (1988) used total 69 different organic compounds to promote the growth of *Aeromonas hydrophila* in drinking water. Compared with carbohydrates, carboxylic acids, and long-chain fatty acids, the cocktail containing 21 amino acids had the highest bacteria growth rate and colony forming units (CFU) at different concentration levels. Both van der Kooij et al. (1992) and LeChevallier et al. (1993) suggested that the AOC is an important indicator for the potential growth of heterotrophic bacteria. Miettinen et al. (1997) found that phosphate is correlated with the bacterial growth measured by HPC for both surface water and groundwater in Finland where AOC does not have a strong correlation with bacterial growth. Sathasivan and Ohgaki (1997; 1999) also indicated that the limited nutrient in Tokyo metropolitan drinking water distribution system is phosphate. The significant growth and the degradation of amino acids were observed by Gagnon and Huck (2001) in the investigation of the removal of easily biodegradable organic matters in biofilm reactor.

In this study, three amino acids (alanine, phenylalanine, and tryptophan) with phosphate were used as the substrate supplements for the filtered-flocculated water from the drinking water treatment plant to test the feasibility of amino acids for promoting bacterial growth in water.

3.2 Materials and methods

3.2.1 Water treatment plant description and source water

The water for this study was sampled from the effluent of the flocculation tank in J.D. Kline Water Supply Plant (JDKWSP) located in Halifax, Nova Scotia, Canada. JDKWSP is a direct filtration water treatment plant with a designed capacity of 227 ML/day. The source water for this water treatment plant is drawn from Pockwock Lake, which can be characterized as low-turbidity, low alkalinity, low-pH, and low-TOC (Vadasarukkai et al., 2011; Knowles et al., 2012). The schematic of JDKWSP is shown in Figure 3.1.

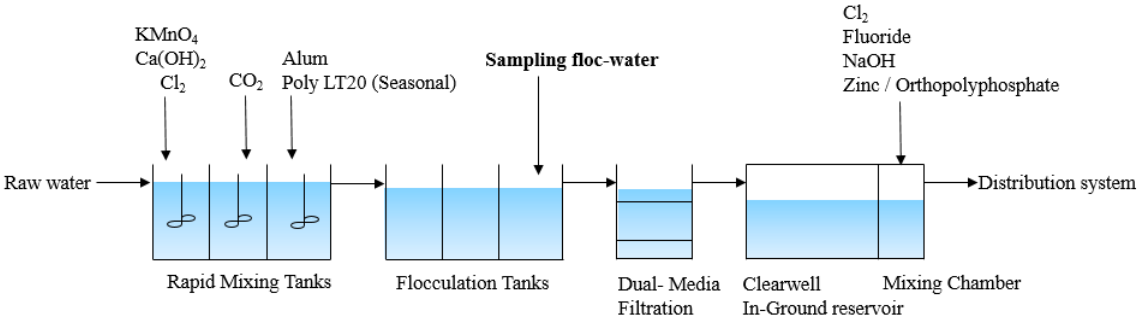

Figure 3.1 Schematic of J.D. Kline Water Supply Plant, Halifax, Nova scotia, Canada.

The water is drawn into rapid mixing tanks where the calcium hydroxide ($Ca(OH)_2$) is added to change low-pH for pH adjustment. Potassium permanganate ($KMnO_4$)is added for the oxidation of metal (i.e., iron and manganese) with the pH 9.6-10 (Knowles et al., 2012). Then carbon dioxide (CO_2) is added to adjust water to pH 5.5-6.0 for the following coagulation (Halifax Water, 2014). When water passes through the final premix tank, aluminum sulfate ($Al_2(SO_4)_3$) is added, and cationic polymer is added as a flocculation aid during the cold winter. After rapid mixing tanks, water goes through flocculation tanks where flocculated water was taken for this experiment. Then water enters the dual media

anthracite-sand filter. After filtration, water is stored in clearwells and reservoirs. Before being delivered into the distribution system, water finally passes a passive mixing chamber where chlorine gas is added for the disinfection, fluoride is added for dental health, sodium hydroxide (NaOH) is added for pH adjustment, and zinc and ortho-polyphosphate are added for corrosion control in the distribution system.

3.2.2 Experimental set-up and design

The batch experimental set-up is shown in Figure 3.2.

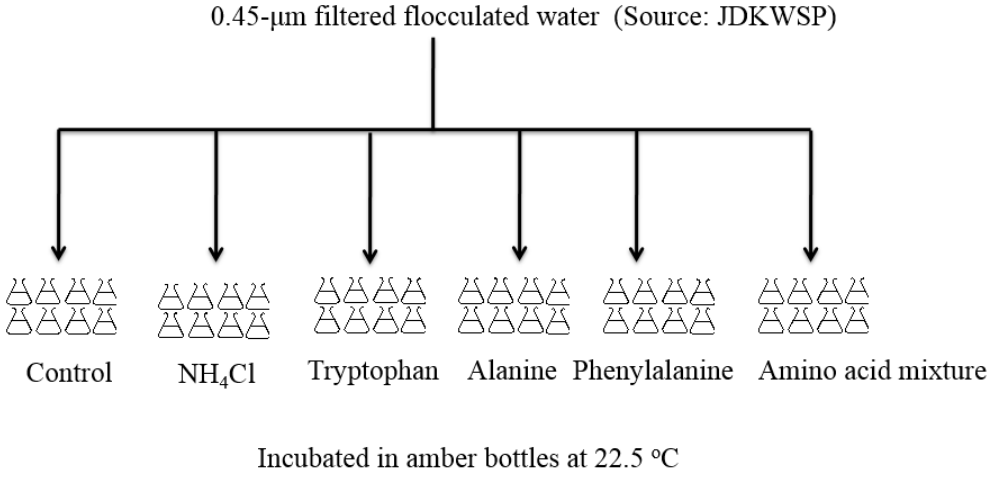

Figure 3.2 Batch experiment of filtered flocculated water with amino acids.

The flocculated-water samples were stored in the fridge at 4 ℃ within 24 hours. In order to remove the floc particles, the flocculated-water was filtered by a 0.45 μm capsule filter device (GE Healthcare, UK). Then samples (500mL) were dosed with NH_4Cl to test the effect of the addition of nitrogen, and amino acids (alanine, phenylalanine, and tryptophan) (chemical formulas are listed in Table 2.1). These water samples were incubated at 22.5 ℃ in 500 mL glass amber bottles. The bottles were covered by the caps with headspace. The

dosage of alanine, phenylalanine, and tryptophan were 4.16, 3.21, and 3.12 mg/L, respectively. Amino acid mix test water (mixture) was consisted of 1.39 mg/L alanine, 1.07 mg/L phenylalanine, and 1.07 mg/L tryptophan. The NH_4Cl testconcentration was 6.82 mg/L. Potassium-biphosphate (KH_2PO_4) was added to water samples to ensure the N:P ratio was at or above 10:1 to maintain the C:N:P ratio of 100:10:1 in aerobic drinking water treatment (LeChevallier et al., 1991). Samples were collected every 24 hours for TOC and ATP measurement over a 5 day period. The 250mL cocktail from the amber bottles was sampled for the duplicated TOC and ATP measurement every day. Thus, the 500mL cocktail of an amber bottle can be sampled for twice.

3.2.3 Analysis method

TOC

Samples were stored in headspace-free 40 mL vials, preserved at 4 ℃ with pH< 2 by the addition of phosphoric acid. These samples were analyzed with a TOC-V CPH analyzer (Shimadzu, Japan) within 7 days.

ATP

Quench-Gone Aqueous (QGA^{TM}) test kits (LuminUltra Corp., New Brunswick, Canada) were used to measure the biomass ATP of water samples according to the manufacturer's instructions. ATP concentration is quantified by the light produced from luciferin/luciferase enzyme in the presence of Mn iron and O_2. A luminometer (PhotonMaster^{TM}, LuminUltra, New Brunswick, Canada) was used to measure the

intensity of light. The reactions between ATP and the luciferin/luciferase enzyme are shown in Equation 3.1 and Equation 3.2.

$$luciferin + luciferase + ATP \overset{Mg2+}{\Longleftrightarrow} luci\ feryl\ adenylate\ cimplex + pyrophosphate \quad \text{Equation 3.1}$$

$$luci\ feryl\ adenylate\ cimplex + O_2 \rightarrow dehydroluciferyl\ adenylate + light \quad \text{Equation 3.2}$$

3.3 Results and discussion

3.3.1 Degradation of TOC in filtered-flocculated water with amino acids

TOC of filtered flocculated-water was 2.283$\pm$ 0.086mg/L (N=2). C/C_o for control and NH_4Cl test bottles were 0.95 and 0.92, respectively, after incubating for 5 days as shown in Figure 3.3. The low TOC removal percentages in the control test bottle (5.5%) and NH_4Cl test bottle (8.3%) could be due to the low AOC concentration in these test bottles. These removal percentages of TOC were in the range of AOC faction (0.1%-9%) reported in the previous study (van der Kooij, 1982). The rapid degradation of TOC in amino acids test bottles appeared on Day 2. On Day 2, C/C_o for amino acid mixture, phenylalanine, tryptophan and alanine test bottles were 0.64, 0.84, 0.76, and 0.96, respectively.

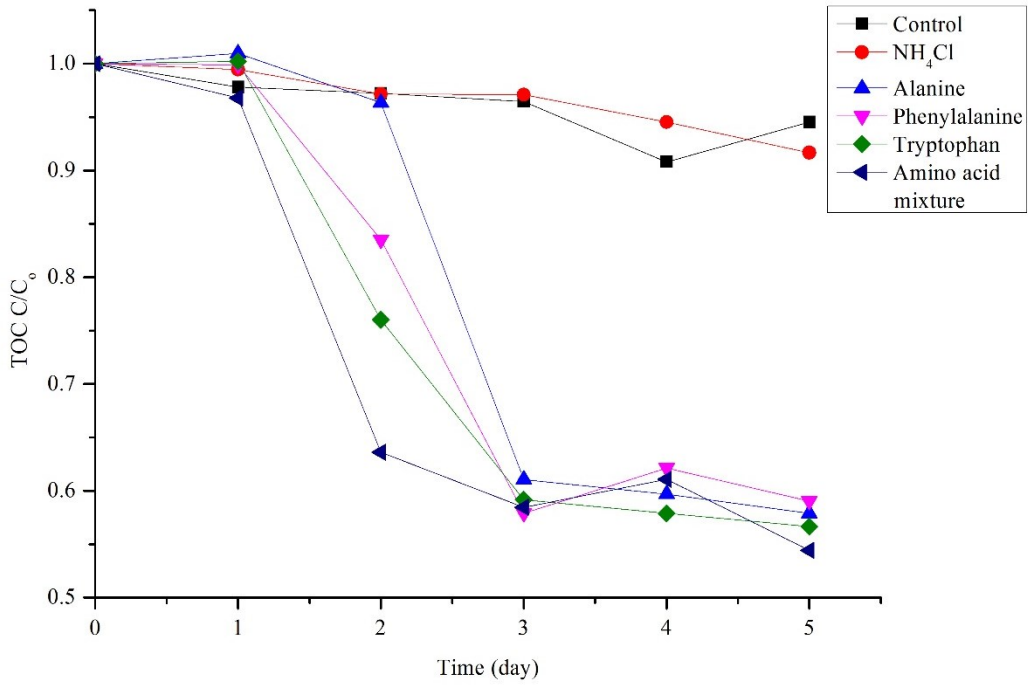

Figure 3.3 TOC removal percentages of filtered flocculated-water versus incubation time.

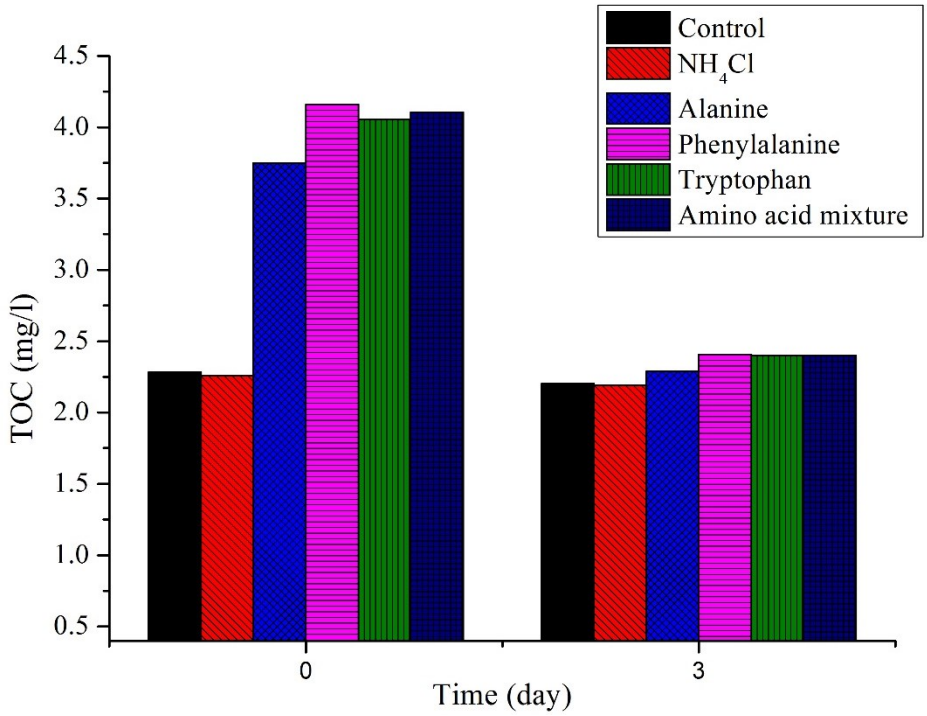

Figure 3.4 TOC concentration versus incubation time.

After 3-day incubation period, the TOC of alanine, phenylalanine, tryptophan and amino acid mixture test bottles were 2.29, 2.41, 2.40, and 2.40 mg/L. TOC of the control test bottle and NH_4Cl test bottle were 2.02 mg/L and 2.19 mg/L. This indicated that amino acids were almost utilized by biomass in water samples. The residual TOC concentration in the amino acid spiked test bottles were slightly higher than TOC concentrations of the control and NH_4Cl test bottle, which may have been caused by the regrowth of bacteria in amino acid test bottles. In previous studies, amino acids were regarded as a portion of AOC and a resource for bacterial regrowth (van der Kooij and Hijnen, 1982; 1988). Gagnon and Huck (2001) also observed the negligible concentration of amino acids (aspartic acid, glutamatic acid, and serine) in the effluent from biofilm reactors. Therefore, amino acids are easily biodegradable organic matters, which can increase the biomass ATP of surface water.

3.3.2 ATP increase in filtered-flocculated water with amino acids

The biomass ATP of test water used in this study was 2.21± 0.04 pg/mL (N=2) caused by the low temperature (4℃) storage condition in the fridge. After 1-day incubation period, biomass ATP of all test bottles were found to be 16 to 53 pg/mL. On Day 2, ATP concentrations of the amino acid test bottles showed an increase while control and NH_4Cl test bottles already reached steady-state.

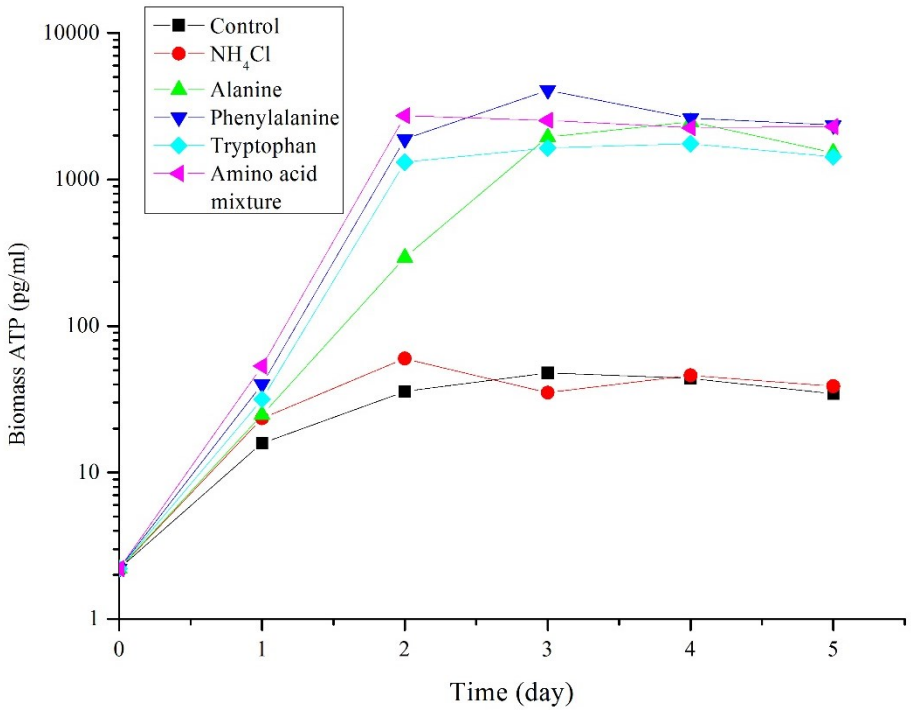

Figure 3.5 Biomass ATP in filtered flocculated-water versus incubation time.

Among the four amino acid test bottles, the maximum biomass ATP of phenylalanine test bottle appeared on Day 3 (4080 pg/mL). Then ATP concentration reached steady at 2400 to 2600 pg/mL in the following days because of the lack of substrate in water samples. A similar trend was observed by van der Kooij and Hijnen (1982) who reported a regrowth of CFU in water samples from waterworks with *P. fluorescens* strain P 17. The steady-state phase in amino acid test bottles was about 48 to 72 hours as shown in Figure 3.5. It could be explained by the rapid degradation of amino acids, the high concentration of amino acids, or the natural microbial consortium in the amino acid test bottles.

The maximum specific growth rates of biomass ATP in test bottles were calculated by Equation 3.4 to 3.8 (Hammes and Egli, 2005)

$$\frac{dN}{dt} = \mu N \quad \text{Equation 3.4}$$

$$\frac{1}{N} dN = \mu \, dt \quad \text{Equation 3.5}$$

$$\int \frac{1}{N} dN = \mu \int dt \quad \text{Equation 3.6}$$

$$N = N_0 e^{\mu t} \quad \text{Equation 3.7}$$

$$\mu = \frac{Ln\,(N) - Ln\,(N_o)}{t} \quad \text{Equation 3.8}$$

Where N is the biomass ATP of water sample (pg/mL);

N_o is the initial biomass ATP of raw sample (pg/mL);

t is the incubation time (h);

μ is specific growth rate (h^{-1}).

Figure 3.6 showed a proliferation of natural microbial consortium in all test bottles during the first 2 to 3 days. The maximum specific growth rates of amino acid test bottles were in the range of 0.094 to 0.148 h^{-1} as shown in Table 3.1.

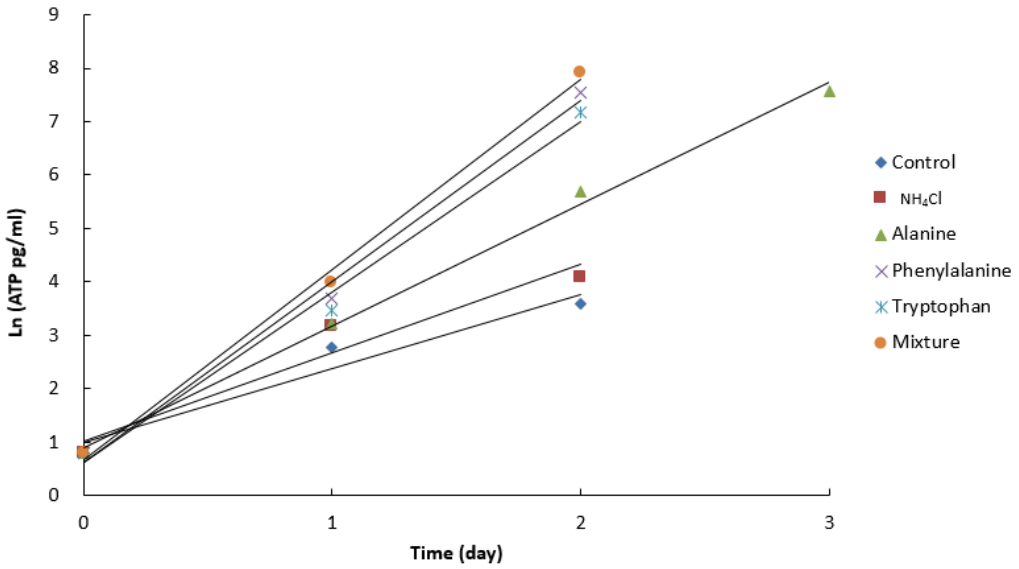

Figure 3.6 Batch growth curves for biomass ATP within 2- or 3-day period.

Table 3.1 Maximum specific growth rate of biomass ATP during 2-3 days.

Water sample	Specific growth rate (h^{-1})	R^2
Control	0.058	0.95
NH_4Cl	0.069	0.94
Alanine	0.094	0.99
phenylalanine	0.141	0.99
Tryptophan	0.133	0.99
Amino acid mix	0.148	0.99

The additional AOC of amino acid test bottles was the major reason for the improvement of maximum specific growth rates. van der Kooij and Hjnen (1988) indicated that amino acid solution had the maximum growth rate of 0.34 h^{-1} and yield value of 8.0×10^6 CFU/µg C which were higher than carboxylic acids, carbohydrates and alcohols and long chain-

fatty acids. Hammes and Egli (2005) reported that the maximum specific growth rate of natural microbial consortium was improved from 0.164 h^{-1} to 0.351 h^{-1} with the additional natural AOC from river water. Therefore, available carbon source can improve the bacterial maximum growth rate. The promotion of maximum growth rates are variable among different carbon sources.

3.4 Conclusion

According to the degradation of amino acids and the increase of ATP concentration, amino acids can be rapidly utilized by the bacteria in treated surface water (filtered flocculated-water). The removal percentage of TOC indicated that the amino acids were totally utilized by bacteria in water samples. AOC is the limited nutrients for bacterial regrowth in this study. As for the nitrogen supplementation, there was no obvious increase in biomass ATP compared with the control test bottle. The increased biomass ATP in amino acid test bottles indicated that amino acid supplementation would result in higher biological activity within a short span of time which may be used to enhance the biological treatment in water treatment processes.

Chapter 4 Enhanced Biofiltration with Amino Acids

4.1 Introduction

Biological activity is regarded as the possible reason for better removal of contaminants in biofilters (Wang el al., 1995), even though the relationship between AOC removal and ATP in normal drinking water biofilters is still unclear (Pharand et al., 2014).Wang et al. (1995) indicated that higher biological activity was possibly correlated with the better removal of NOMs and DBPs precursors. Naidu et al. (2013) observed 90% AOC removal and about 56 % DOC removal with average 51 μg ATP/g media in seawater-fed biofilters.

In order to improve the biological activity in biofilters, phosphate supplementation has been applied in the previous studies (Yu et al., 2003; Sang et al., 2003; Lauderdale et al., 2012; Granger et al., 2014). The suggested C:N:P molar ratio is 100: 10:1 which can satisfy the requirement of bacterial growth in aerobic drinking water treatment (van der Kooij et al., 1982; LeChevallier et al., 1991). However, additional phosphate would break the suggested C:N:P ratio in biofilters. van der Kooij et al. (1988) indicated that amino acids are easily biodegradable organic matters and can improve the bacteria growth. Therefore, amino acids would be the comprehensive supplements for biofilm growth.

This chapter focuses on the increased biological activity (as measure by ATP) of biofilm with amino acids (phenylalanine, tyrosine, and tryptophan) supplements in bench-scale biofilters. In addition, this chapter also focuses on the kinetics study of biomass growth and amino acid degradation. Kinetics of biomass ATP growth is analyzed by Baranyi and

Roberts' growth curve. Kinetics of amino acid degradation (as measure by DOC and peCOD) are analyzed by the first-order kinetics model.

4.2 Materials and methods

4.2.1 Experimental set-up and operation

Four columns were used to investigate the biological activity of biomass and the degradation of amino acids. Phenylalanine, tyrosine, and tryptophan represent compounds having different molecular structures (chemical formulas are listed in Table 2.1). shown in Table 2.1), which may enhance the biological activity of biomass through different metabolic and catabolic pathways (Barker, 1981; Christensen et al., 1999).

The enhanced biofilter setup is illustrated in Figure 4.1.

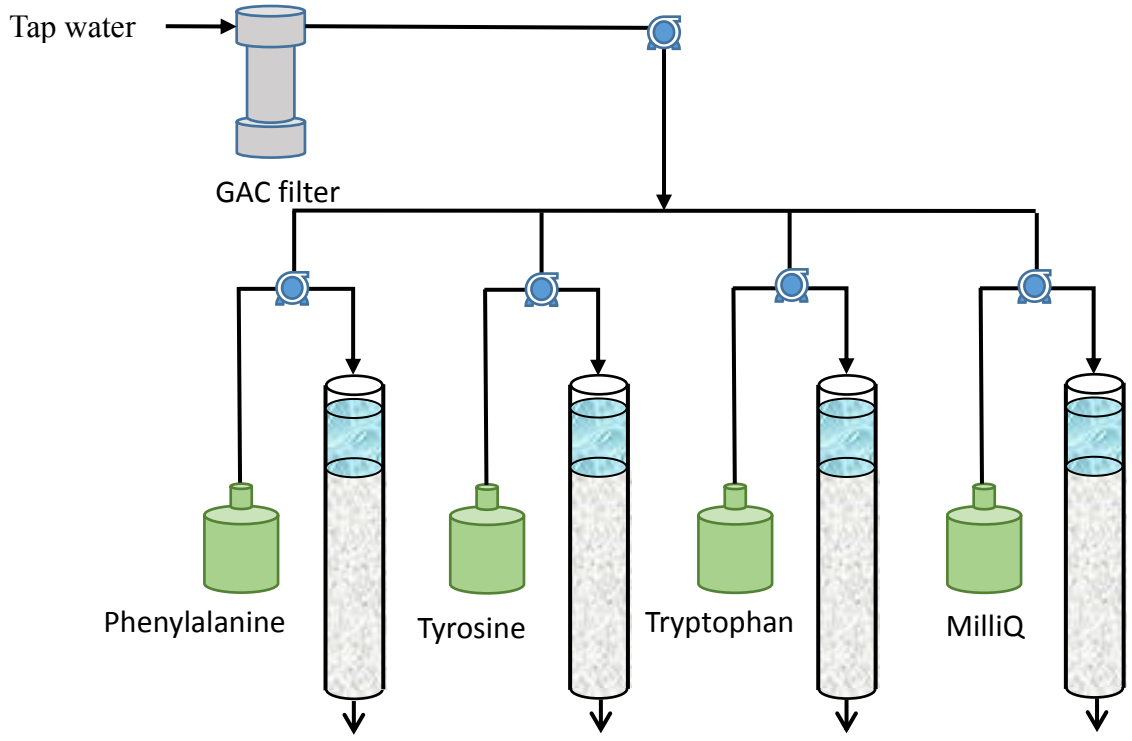

Figure 4.1 Enhanced biofilters setup for determining biological activity on glass beads.

The bench-scale enhanced biofilter set-up consisted of four Kontes Brand chromatography columns (Vineland, New Jersey, USA). Each column (diameter 2.5cm, length 20cm) was filled with 15 cm borosilicate glass beads (diameter was 2 mm; Sigma-Aldrich, USA) over 0.5 cm of gravel stone. Columns were covered with aluminum foil to protect from the light.

Biofilters were fed with dechlorinated tap water from the J.D. Kline Water Supply Plant. A GAC filter was used to remove residual chlorine in tap water. The quality of dechlorinated tap water is shown in Table 4.1. The EBCT of columns was 14 to 15 min, resulting in an influent flow rate of 6.6 L/day per column. Biofilters were operated for 96 hours between backwashes. Reverse osmosis water was pumped by a peristaltic pump into the bottom of column, and glass beads were stirred with a glass stirring rod during backwash.

Phenylalanine, tyrosine, and tryptophan (Sigma-Aldrich, USA) were pumped into three columns. The fourth column fed with MilliQ® water was the control column. Masterflex tubing (Montreal, Canada) and peristaltic pump (Cole-Parmer®, USA) were used to supply amino acids to the biofilters. Amino acids were stored in four 4L sterile amber bottles. Amber bottles were autoclaved before filling up with stock solution. The target concentration of amino acids was 3 mg/L with 0.32 to 0.38 mg/L phosphate (shown in Table 4.1) in the influent. Biofilters were operated for one month before the experiment to reach steady state.

Table 4.1 Quality characteristics of dechlorinate tap water for biofilters.

Experimental condition	Data Range (N=2)
DOC (mg/L)	1.82 ± 0.15
pH	6.8 ± 0.1
DO (mg/L)	10.41 ± 0.13
Water temperature (℃)	11.5 ± 0.7
Phosphate * (mg/L)	0.35 ± 0.04
Alkalinity (mg/L)	23.51 ± 1.63

*Halifax Water add ortho-polyphosphate to control the corrosion in distribution system.

4.2.2 Analysis methods

ATP

Deposit & Surface Analysis (DSA^{TM}) test kits (LuminUltra, New Brunswick, Canada) were used to determine the biological activity of biofilm grown on glass beads according to the manufacturer's instructions. This analysis method involves chemical removal of biofilm from filter media, reaction with luciferin/luciferase enzyme, and quantification of the emitted light using a luminometer (PhotonMaster^{TM}, LuminUltra, New Brunswick, Canada).

DOC

Water samples were filtered through a preconditioned 0.45 μm polyethersulfone (PES) filter membrane and stored in headspace-free 40 mL vials, preserved at 4 ℃ with pH< 2

by addition of phosphoric acid. These samples were analyzed with a TOC-V CPH analyzer (Shimadzu, Japan) within 7 days.

PeCOD

Water samples were filtered through a preconditioned 0.45 μm PES filter membrane and preserved at 4 ℃ with pH< 2 by addition of concentrated sulfuric acid. These samples were measured using a PeCOD® L100 AssayPlus™ analyzer (Mantech Inc., Guelph, Canada) within 2 days after neutralizing to pH 7.0 with concentrated sodium hydroxide. The dilution caused by sulfuric acid and sodium hydroxide solutions was negligible. Samples were analyzed as described by Stoddart and Gagnon (2014).

Fluorescence spectroscopy

A fluorometer (Horiba Scientific, New Jersey, USA) was used to generate the fluorescence excitation-mission matrices (FEEMs) of filtered water samples. The fluorometer has an excitation wavelength range of 230 to 610 nm and an emission wavelength range of 250 to 620 nm. The integration interval was 0.1 nm and the spectral resolution was 3 nm. MilliQ® water was used as a blank to measure the signal to noise ratio and to evaluate the performance of the xenon lamp (Trueman et al., 2016). After generating data, the FEEMs were normalized by removing the inner filter effect and both 1st and 2nd order Raleigh scattering, as described by Trueman et al. (2016). Multi-way parallel factor analysis (PARAFAC) was implemented using N-way tool box (Andersson and bro, 2000) in MATLAB 7.12.0 (MathWorks, Natick, MA, USA).

Biomass growth curve

Biomass on the top layer of columns was simulated by the first order differential equation described by Baranyi and Roberts (1994). Stoddart et al. (2016) applied this equation to investigate biomass ATP in full-scale drinking water biofilters. The model is described by Equation 4.1. Biomass ATP was used for the model instead of cell concentration. This substitution is supported by previous studies. Delahave et al. (2003) reported a linear relationship between log (ATP) and log (HPC) in surface water. Magic-Knezev and van der Kooij (2004) showed that ATP was correlated with total direct bacterial cell counts in GAC filters. Dowdell (2012) indicated a linear relationship between biomass ATP and phospholipid biomass.

$$y(t) = y_0 + \mu_{max}t - \frac{1}{m}\ln\left(1 + \frac{e^{m\mu_{max}t} - 1}{e^{m(y_{max} - y_0)}}\right) \qquad \text{Equation 4.1}$$

Where $y(t)$ is natural logarithm of cell concentration at the time *t*;

y_o is natural logarithm of the initial cell concentration, $y(t) = y(0)$;

μ_{max} is the maximum specific growth rate;

y_{max} is natural logarithm of maximum population density;

m is a curvature parameter for sigmoid growth mode.

The data were inputted into ComBase DMFit (ComBase, 2015) to generate the results.

4.3 Results and discussion

4.3.1 Biomass growth

4.3.1.1 Biomass with backwash cycles

Servails et al. (1991; 1994) observed a vertical variation of biomass in GAC filters above 9 ℃, where bacterial biomass was seen in the range of 2.5 to 10.9 μg C/cm^3. Wang et al. (1995) observed that biomass attached to the top layer of filter media was always the highest and biomass concentration decreased as depth increased. The vertical stratification usually appeared at high temperatures (≥15℃) not at lower temperatures (Servails et al.,1991; 1994). Therefore, biological activity of biomass attached to top layer of filter media is a good indicator for evaluating overall biological activity in this study (water temperature was 11 to 12℃).

To understand the increase in biological activity, filter media (glass beads) was taken every day to measure the biomass ATP within 3 backwash cycles. In addition, media was taken before and after backwash to determine the biomass lost during the backwash. Biomass ATP on the top layer of filter media versus operation time is shown in Figure 4.2.

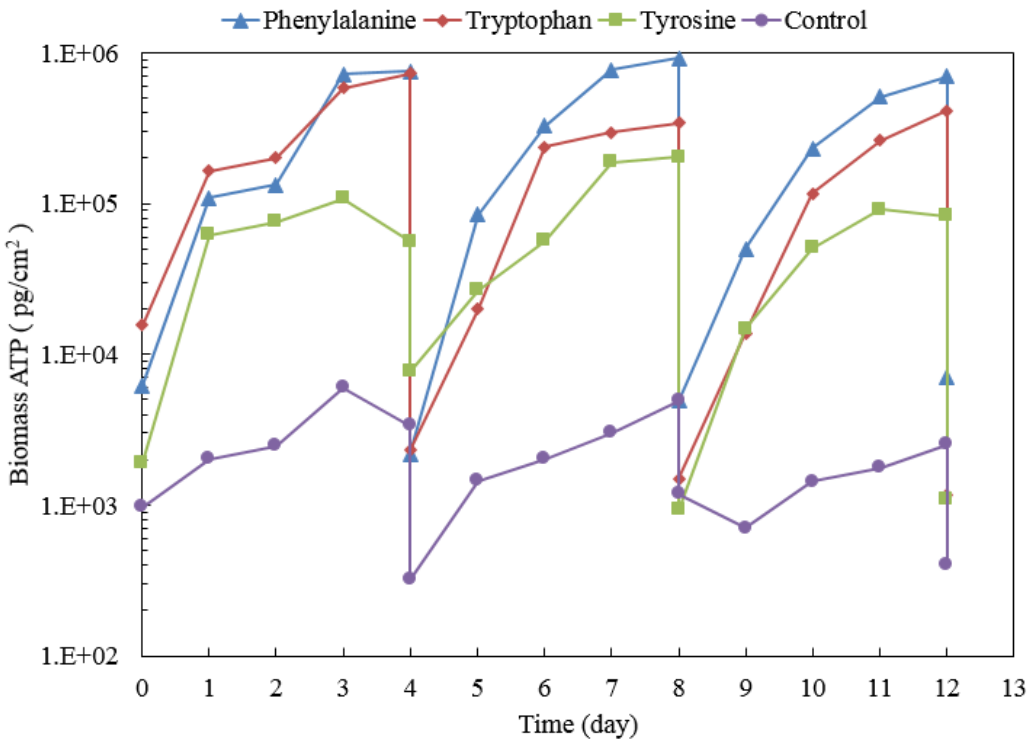

Figure 4.2 Biomass ATP of media versus operation time.

In control column, biomass ATP was 3.2×10^2 to 1.2×10^3 pg/cm^2 at the start of the filter cycle and 2.5×10^3 to 4.9×10^3 pg/cm^2 at the end of filter cycle. This can be explained by the low AOC in dechlorinated tap water, because the tap water had been treated by the pilot-scale biofilters in J.D. Kline Water Supply Plant. In addition, previous studies also indicated that the low AOC fraction in DOC was only 0.1 to 0.9 % in surface water (van der Kooij, 1982; Hammes and Egli, 2005). Therefore, the low concentration of AOC in the feeding water was the major reason for the low biomass growth rate in control column.

All three amino acid-supplemented columns demonstrated a significant promotion of biological activity. Phenylalanine- and tryptophan-supplemented columns achieved almost the same level of biomass ATP. Biomass ATP of phenylalanine-supplemented column at

the end of filter cycle was 6.9×10^5 to 9.2×10^5 pg/mL and biomass ATP of tryptophan-supplemented column at the end of filter cycle was 3.4×10^5 to 7.2×10^5 pg/cm^2. At the same target concentration (3mg Amino acid /L), biomass ATP of the tyrosine-supplemented column was not as high as that of phenylalanine- and tryptophan-supplemented columns. Biomass ATP of the tyrosine-supplemented column at the end of filter cycles was 5.5×10^4 to 2.02×10^5 pg/cm^2. These results demonstrated that amino acids have a great potential for improving biological activity in biofilters within a very short span of time.

4.3.1.2 Biomass growth with respect to predicting model

The rapid increase in biomass ATP on the top layer of biofilters was observed within three filter cycles. To simulate multiplication of biomass ATP, a first order differential equation (Baranyi and Roberts, 1994) was applied to estimate growth parameters. The model and measured data within 100 hours are shown in Figure 4.3. The model parameters are shown in Table 4.3.

Velten et al. (2011) suggested two equations to determine the specific growth rates of biomass (μ_{max}) in biofilters before the stationary phase and yield (biomass production/ DOC removal) at stationary phase over a 198-day period. Comparatively, the sigmoidal growth curve developed by Baranyi and Roberts (1994) is better to describe the change of biomass ATP at both lag phase and stationary phase over a short period (100-hours).

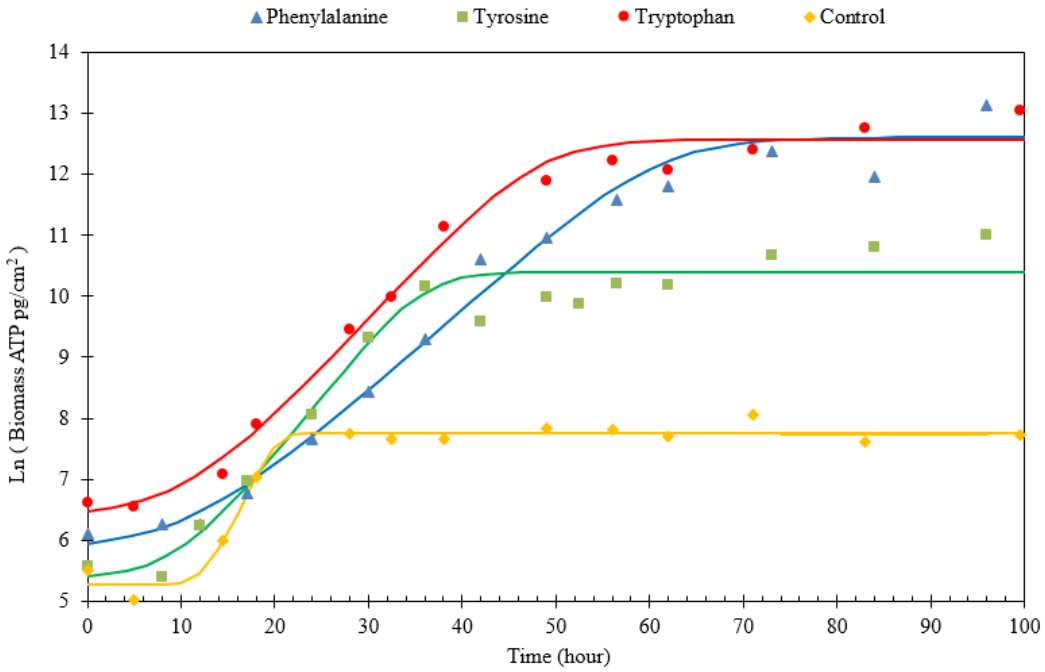

Figure 4.3 Evolution of measured biomass concentration in the biofilter with estimated growth model for each amino acid condition.

Table 4.2 Model parameters for evolution of biomass concentration in one filter cycle.

Feeding water	Avg. initial value (Ln ATP pg/cm^2)	Avg. lag (h)	Avg. maximum specific growth rate (h^{-1})	Avg. final value (Ln ATP pg/cm^2)	R^2
Influent +Phenylalanine	5.94	11.46	0.135	12.61	0.98
Influent +Tyrosine	5.41	9.50	0.189	10.40	0.95
Influent +Tryptophan	6.47	10.33	0.161	12.57	0.98
Influent +MilliQ	5.27	12.29	0.311	7.74	0.98

Throughout this section, the value of initial value (y_0) and final value (y_{max}) in the model is always taken to be its natural logarithm. Measured biomass ATP was in good agreement

with the Baranyi and Roberts' growth curve. R^2 was above 95% for all four columns. The biomass ATP at the start of filter cycle in four columns were 5.27 to 6.47, which was corresponded to about 190 to 640 pg/cm^2. This indicated that biomass had been removed by the backwash. Because glass beads have a relatively small specific surface area (30 cm^{-1}) and smooth surface, attached and accumulated biomass was easily removed. Specific growth rates of amino acid-supplemented columns were 0.135 h^{-1} (phenylalanine), 0.189 h^{-1} (tyrosine), and 0.161 h^{-1} (tryptophan). The tyrosine-supplemented column had the highest specific growth rate, but y_{max} was 10.40 (about 3.2×10^4 pg/cm^2). Even though phenylalanine and tryptophan supplementations achieved the lower specific grow rates. y_{max} values of phenylalanine- and tryptophan-supplemented columns were 12.61 (about 2.9×10^5 pg/cm^2) and 12.57 (about 2.8×10^5 pg/cm^2), respectively. Therefore, specific growth rate was not correlated with biomass ATP at stationary phase.

4.3.1.3 Biomass penetration through the depths of the biofilter

Biomass ATP of the top layer is a good indicator of the whole biomass and biological activity in biofilters. The vertical variations of biomass ATP were reported by Dowell (2012), Pharand et al. (2013), and Rahman (2013). Servails et al. (1991; 1994) reported a seasonal variation of biomass in term of depths and vertical variation of biomass measured by respiration of ^{14}C. Wang et al. (1995) also observed a decreased biomass concentration measured by phospholipid as depth of biofilter increased. For phosphorus enhanced biofilters, phospholipid and oxygen uptake rate (OUR) of biofilm decreased as depth increased (Sang et al., 2003)

For bench-scale biofilters, samples of different depths cannot be taken during the filtration cycle, because the sampling would break filtration function and rearrange the filter media at different depths. In this study, biomass taken at different depths were sampled at 120h as shown in Figure 4.4 a-d. Sample results indicated that the biomass ATP declined logarithmically with depths.

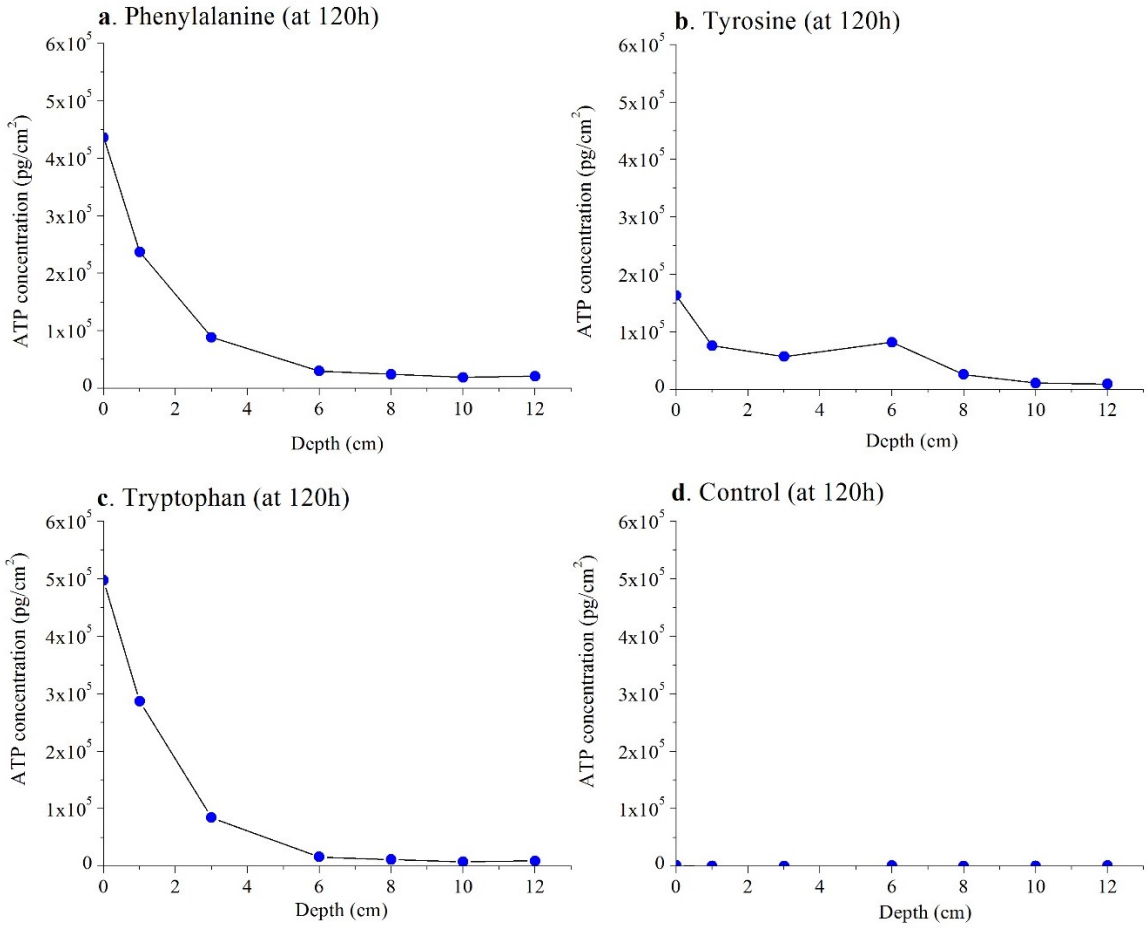

Figure 4.4 a-d Biomass ATP at stationary phase (120h) versus media depths.

The curves of biomass ATP were different in four columns. Velten et al. (2011) investigated DOC removal at different depths in GAC biofilters over 198 days, which indicated that the high adsorption capacity of fresh GAC leads to the rapid biofilm

development in the upper layer of filter media. This vertical variation was also observed in these four columns. Even though the adsorption capacity of glass beads was negligible, the high concentration of amino acids at the top layer resulted in the increase in biological activity of biomass. Meanwhile, the increased biological activity improved degradation of amino acids in the upper layer.

The depth distribution showed the difference in total amount of biomass grown on the filter media with different amino acid supplements at the same target concentration. This phenomenon indicated different types of amino acids would result in different promotions of biological activity.

4.3.2 Degradation of substrate

4.3.2.1 Degradation of DOC and PeCOD

The utilization of three amino acids in biofilters were very rapid. The results showed that DOC and peCOD removal ceased within a backwashing cycle. The steady state was defined as the period when DOC or peCOD concentration did not have a significant change. DOC of effluent at steady state was almost the same as the dechlorinated tap water, which indicated that no amino acids were left. This means amino acids had been rapidly utilized by the biofilm and would not result in a residual problem of organic carbon in the effluent.

However, there was a difference between these DOC and peCOD removal. The results demonstrated that removal percentage of DOC was lower than that of peCOD. The average removal percentage of peCOD in the phenylalanine-supplemented, tyrosine-supplemented,

tryptophan-supplemented, and control columns were about 64, 63, 51, and 23 %, respectively, at the steady-state (Figure 4.5). The average removal percentage of phenylalanine-supplemented, tyrosine-supplemented, tryptophan-supplemented, and control columns as measured by DOC were about 42, 38, 43, respectively, at the steady-state (Figure 4.5). Shin and Lim (1996) reported that the COD/TOC ratio of effluent (2.406) was lower than that of influent (2.800) in an investigation of microbial decomposition of aquatic fulvic acid.

Considering biomass ATP growth curves, peCOD may be a better indicator than DOC to assess the operational performance of biofilters.

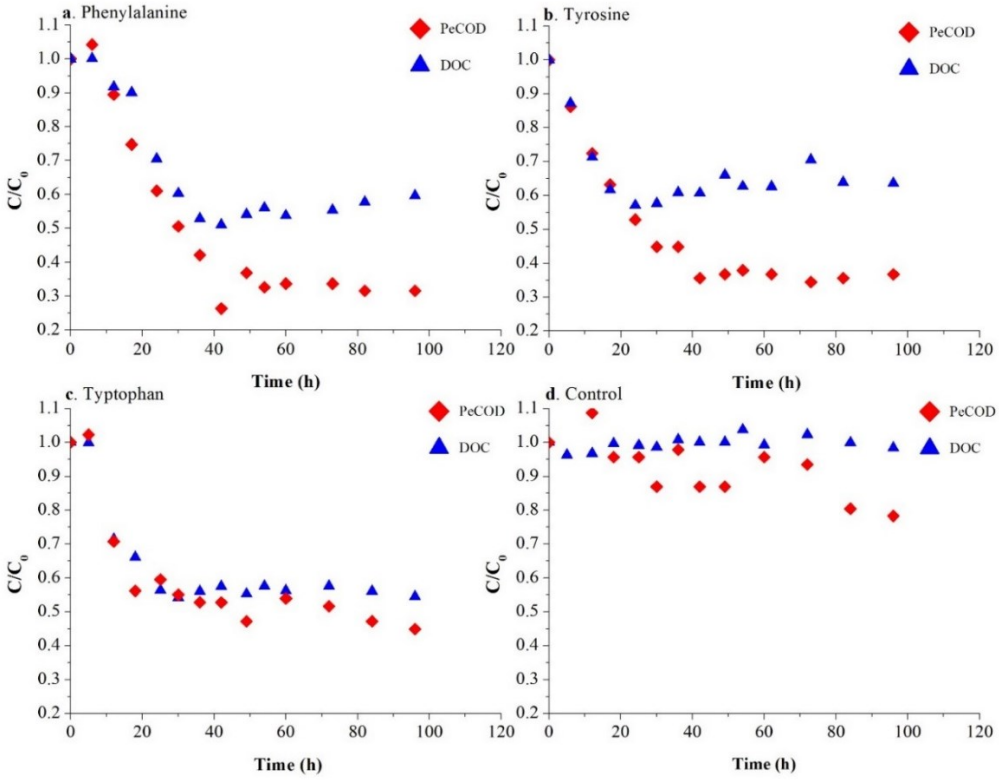

Figure 4.5 a-d C/C_0 of DOC and peCOD in effluent versus operational time.

There was a longer degradation time of water samples measured by peCOD than by DOC, which was almost the same as the time of ATP growth (Figure 4.3). Therefore, a better sensitivity of peCOD in assessment of biofilters' performance was indicated in terms of the greater substrate removal, ATP growth phase, and degradation time of peCOD.

4.3.2.2 Fluorescence excitation-emission matrix

The model of two compounds was applied to analyze FEEMs of effluent with PARAFAC analysis method. The one compound represented NOMs in the feeding water and the other one represented amino acids as shown in Figure 4.6 a-b. The signal of phenylalanine was unclear because of its weak fluorescence characteristic. Therefore, these is no figure about FEEMs of phenylalanine. For control column, this model divided NOMs of dechlorinated tap water into two NOM compounds (shown in Figure 4.6 c).

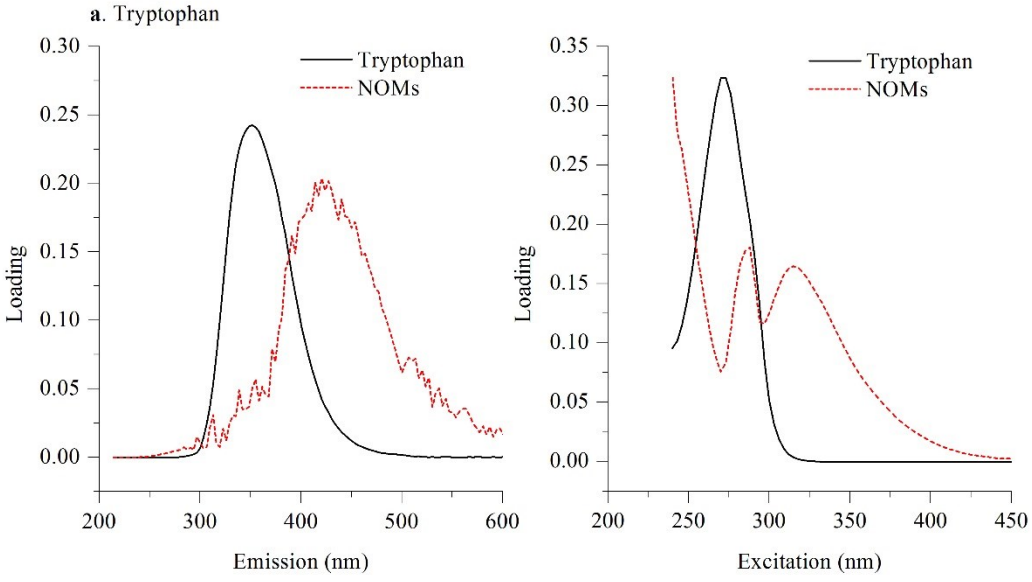

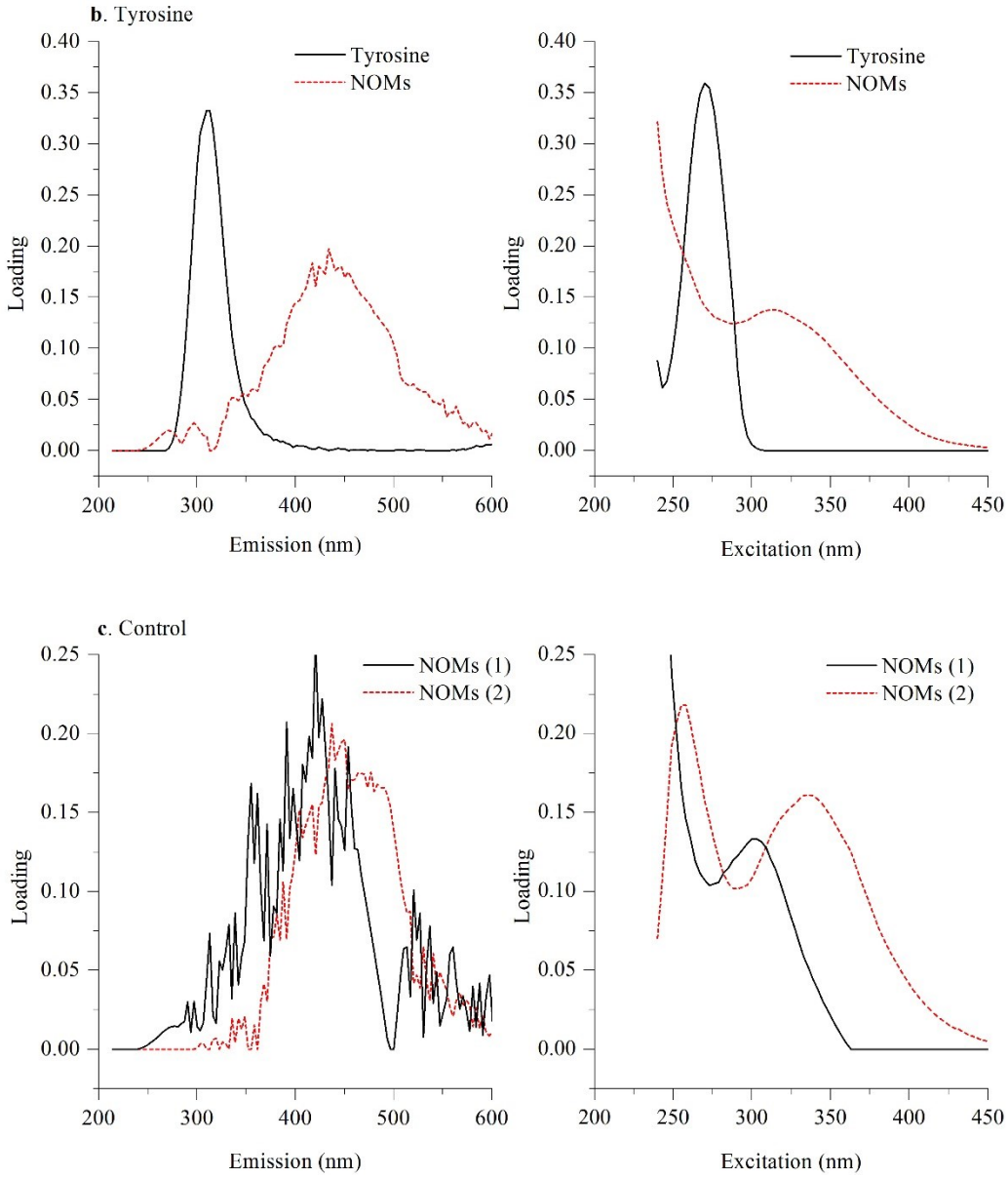

Figure 4.6 a-c Emission loading and excitation loading

The maximal level of fluorescence was selected to represent the concentration of amino acids and NOMs as shown in Figure 4.7. FEEMs data confirmed that amino acids are easily biodegradable in biofilters. After operating 20 to 40 hours, there was no signal of amino acids, which meant amino acids had been completely removed by biofilters. Except for the control column, possible NOMs removal was observed in amino acid columns.

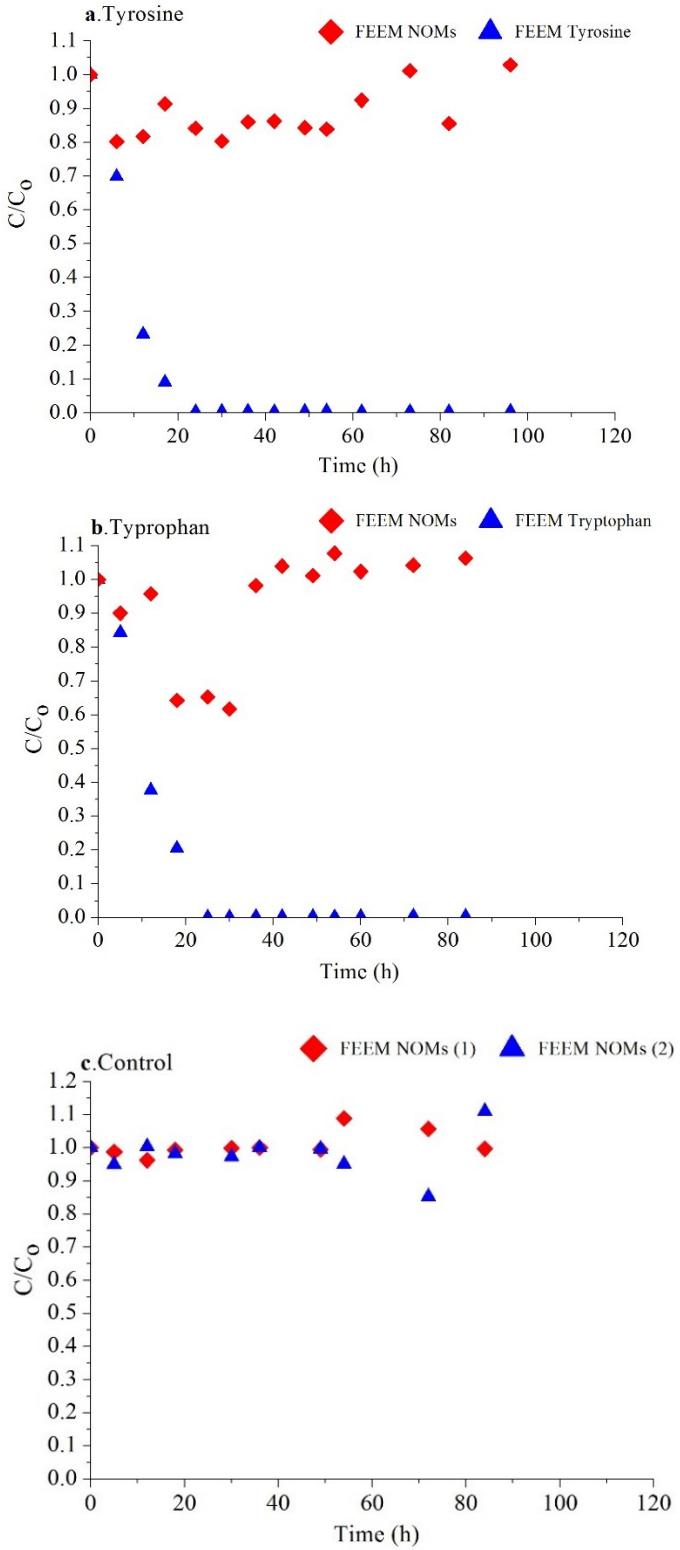

Figure 4.7 a-c C/Co of FEEMs in effluent versus operational time.

It is noted that the feeding water had been run through the biofilters in J.D. Kline Water Supply Plant (Figure 3.1). Thus, the biodegradable organic matters fraction in feed water was pretty lower. Therefore, FEEMs of NOMs may not provide the strong evident to demonstrate the removal of NOMs, because several factors may result in measurement error, such as fluctuation of water quality from the network, mathematic analysis method, and signal interaction of FEEMs. On the other side, the increased biological activity may be useful for removing NOMs. Therefore, more future studies are required to examine whether biomass enhanced by amino acids is able to improve NOMs removal.

4.3.2.3 Kinetics of substrate degradation

Many theoretical and empirical kinetic models have been reported in previous studies to describe the biodegradation of organic compounds in drinking water. In this study, a first-order kinetic model was applied to determine the kinetics of amino acid biodegradation (Equation 4.2 and Equation 4.3)(Mihelcic and Zimmerman, 2014).

$$r = \frac{-dC}{dt} = kC \qquad \text{Equation 4.2}$$

$$\ln(C) = \ln(C_o) - kt \qquad \text{Equation 4.3}$$

Where r is rate of degradation of substrate, mg/L.h;

k is the specific rate of substrate degradation, h^{-1};

C is the measured concentration of substrate, mg/L;

C_o is the initial concentration of substrate, mg/L;

t is the operational time, h.

The kinetic parameters of DOC removal and peCOD removal are shown in Figure 4.8.

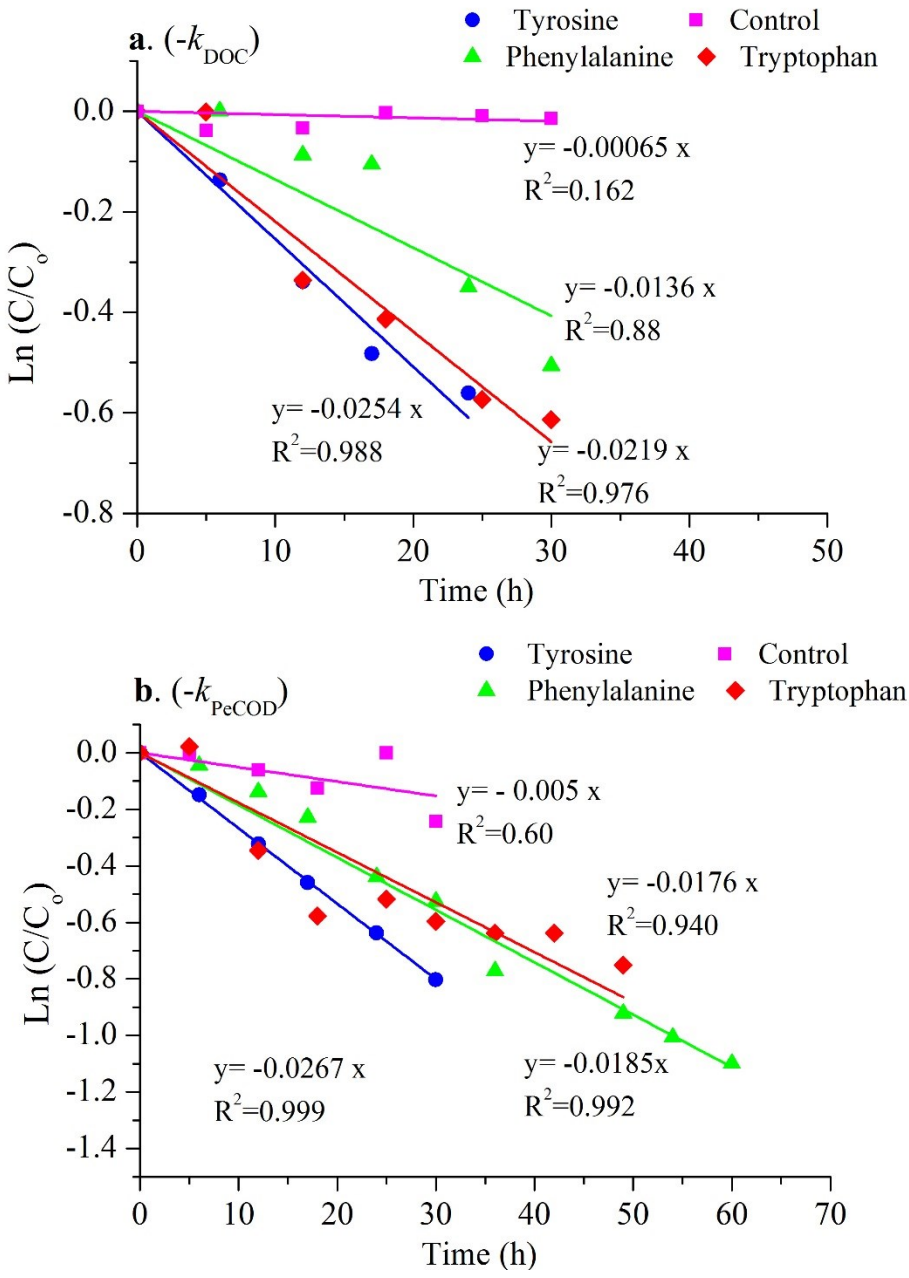

Figure 4.8 Kinetics of DOC removal (top figure) and peCOD removal (bottom figure).

k_{DOC} for phenylalanine, tyrosine, and tryptophan were 0.0136, 0.0254, and 0.0219 h^{-1}, respectively. For amino acid supplemented columns, k_{peCOD} of phenylalanine, tyrosine

and tryptophan were 0.0185, 0.0267, and 0.0176 h^{-1}, respectively. The k_{peCOD} of control column was 0.005 h^{-1} while $k_{\mathrm{DOC}}$of control column was almost 0.

The $k$values for DOC and peCOD were slightly different in both amino acid-supplemented columns and the control column. Compared with biomass ATP growth curve of amino acid-supplemented columns as shown in Figure 4.3, k values were correlated with maximum specific growth rates. Tyrosine had the highest k values for both DOC and peCOD removal with the highest maximum specific growth rate (0.189 h^{-1}). k_{DOC} of tryptophan and phenylalanine also indicated that maximum specific growth rate of tryptophan was higher than phenylalanine. For peCOD removal, in 0 to 30 h, Ln (C/C_o) of tryptophan was lower than phenylalanine which indicated that maximum specific growth rate of tryptophan was higher than phenylalanine. However, there was no significant difference in k_{peCOD} of tryptophan and phenylalanine. This can be ascribed to measurement error at low COD concentration or tryptophan supplementation could not improve the oxidation capacity for background COD.

In addition, biodegradation time of peCOD was longer than biodegradation time of DOC (Figure 4.5; Figure 4.8). This means the biological oxidation was still going on when DOC removal creased. Compared with the model curves of biomass ATP (Figure 4.3), the peCOD data were better to fit the exponential and stationary phases of biomass ATP growth in amino acid-supplemented columns. This confirmed that peCOD is a better indicator for substrate biodegradation to couple with biomass ATP, rather than traditional DOC measurement.

4.4 Conclusion

Bench-scale biofilters study demonstrated that amino acids are easily biodegradable compounds and can increase biological activity of biofilm. At the same target concentration, amino acids resulted in different promotions of biological activity in biofilters. Baranyi and Roberts's growth curves demonstrated that there was no relationship between maximum biofilm growth rates at exponential phase and final biomass ATP levels at stationary phase, because the duration of the exponential phases were different.

A first order kinetic model was applied to determinate the degradation of amino acids within one filter cycle. FEEMs of effluent demonstrated that there was no amino acid residuals in effluent after operating more 40 hours. In addition, peCOD is an appropriate substrate indicator to couple with biomass ATP at the exponential and stationary phases.

Chapter 5 Kinetics of Amino Acids in CDC Biofilm Reactors

5.1 Introduction

Biofiltration involves both biological treatment (biofilm) and filtration functions. This chapter focuses on the kinetics of amino acid degradation and biomass growth as measured with ATP in biofilm reactors, without the filtration function. Huck et al. (1994) suggested a first-order model for biodegradable organic matter (BOM) removal in full-scale biofilters. For drinking water biofilm, Gagnon (1997) indicated that neither internal nor external mass transfer limit BOM removal in drinking water biofilm. In this study, the purpose was to analyze the utilization rates of amino acids and the conversion efficiency from amino acids to biomass ATP using the kinetic models described by Rittmann and McCarty (2001) and Gagnon and Huck (2001).

5.2 Materials and methods

5.2.1 Experimental set-up and design

The CDC biofilm reactor is shown in Figure 5.1. The bench-scale setup consisted of a CDC biofilm reactor (BioSurface Technologies, Montana, USA) and a 18L sterile glass jug with amino acid stock solution. Masterflex tubing (Montreal, Canada) and a peristaltic pump (Cole-Parmer®, USA) were used to feed the biofilm reactors. The glass jugs were autoclaved every week and covered by a paper box to protect from the light.

Three CDC biofilm reactors were covered with aluminum foil to protect from the light. The rods and baffle displaced approximately 50 mL of solution. The effluent spout at 400

mL resulted in a volume of solution approximately 350 mL as shown in Figure 5.1. Eight polypropylene rods held 24 polycarbonate coupons (a diameter of 1.27 cm and a thickness of 0.3cm). The estimated surface area of biofilm reactor was 621 cm^2. To minimize degradation of amino acids caused by suspended biomass, hydraulic retention time (HRT) of reactor was 30 min (flow rate was 16.8 L/day) to flush out suspended biomass in bulk water.

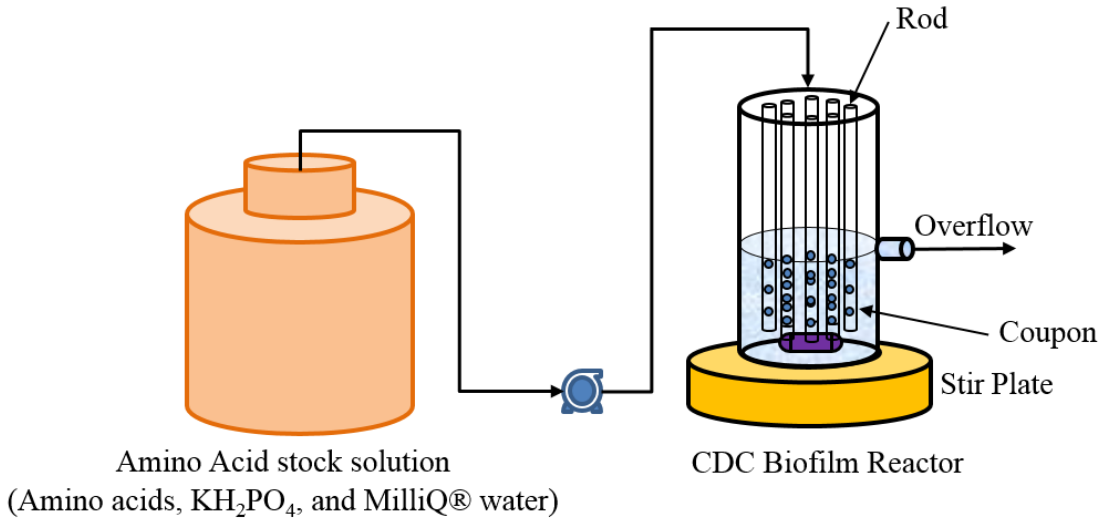

Figure 5.1 Schematic diagram of CDC biofilm system.

To incubate the biofilm on coupons, three reactors were fed dechlorinated tap water from the J. D. Kline Water Supply Plant in Halifax, Canada (water quality is shown in Table 4.1) for two weeks. After two weeks of operation, the influent was replaced with the stock cocktails consisting of amino acids (tyrosine, phenylalanine, and tryptophan), potassium-biphosphate (KH_2PO_4) and MilliQ® water. The target concentration of amino acids was in the range of 0.02 to 2.0 mg/L. To ensure good performance of biological treatment in

biofilm reactor, the C:P ratio in influent was controlled as approximately 100:1. Reactors were run at certain concentration levels of amino acids at least 1 week before each sampling to ensure the biofilm achieve stationary phase.

5.2.2 Analysis methods

Biological activity

Deposit & Surface Analysis (DSA^{TM}) test kit (LuminUltra, New Brunswick, Canada) were used to measure biomass ATP on the surface of polycarbonate coupons according to the manufacturer's instructions. Polycarbonate coupons were taken from polypropylene rods without scraping the surface. The coupons was immersed and stored in the extraction solution of the DSA^{TM} test kits. Samples were measured within 1 hour.

Liquid Chromatography-Mass Spectrometry (LC-MS)

The LC-MS analysis was performed by a combination of high performance liquid chromatography (HPLC) with mass spectrometry (MS). The HPLC system, from Agilent 1260 binary pump was used for all analytes. An Agilent Zorbax Eclipse plus C-18 RRHD (2.1 X 50 mm, 1.8 μm) column was used for chromatographic separation of all analytes. The column was maintained at 25 °C throughout the run. The mobile phase comprising of water with 0.1% formic acid (A) and methanol (B) at 0.33 mL/min was used for separation. 5uL of sample was injected through the column. The gradient at 10% B was initially held and the solvent B was linearly increased to 40% till 3.40 min. A post-time of 3.30 min was added to allow the column to re-equilibrate before the next analysis. This resulted in a total cycle time of 7.7 min.

Mass spectrometry was performed on an Agilent 6460 triple quadruple mass spectrometry. Details of optimized compound-specific parameters and optimized MS sources are shown in Table 5.1 and 5.2. The mass spectrometer was run in multiple reaction monitoring (MRM) mode in electrospray ionization (ESI) positive. Two transitions: a quantifier (most abundant product) and qualifier were used for most of the compounds to increase specificity of the method. Data acquisition and analysis was performed using Agilent MassHunter software (version Rev B.08.00).

Table 5.1 Optimized compound-specific parameters and retention time for LC-MS/MS.

Amino acids	Precursor Ion (m/z)	Product Ion (m/z)	Dwell	Fragmentor (V)	Collision energy (V)	Cell accelerator voltage (V)	Retention time (min)
Tyrosine	182.1	165 (136)	35	94	6 (10)	4	1.2
Phenylalanine	166.1	120 (103)	35	77	10 (3)	4	2.1
Tryptophan	205.1	188 (146)	35	89	6 (14)	4	2.7
Caffeine	195.1	138 (42.2)	35	126	17 (40)	4	3.1

Table 5.2 Optimized source parameters of mass spectrometer.

Parameter	ESI Positive
Gas temperature (°C)	300
Gas flow rate (L/min)	5
Nebulizer (psi)	60
Sheath gas temperature (°C)	300
Sheath gas flow (L/min)	11
Capillary voltage (V)	4000
Nozzle voltage (V)	2000
Delta EMV (V)	400

5.3 Results and discussion

5.3.1 Description of biofilm model

The model of steady-state thin biofilm is presented in Figure 5.2.

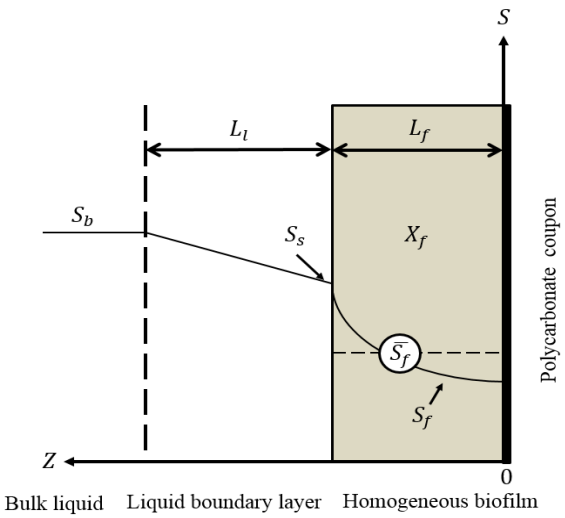

Figure 5.2 Model of steady-state thin drinking water biofilm with utilization of substrate (Gagnon and Huck, 2001).

It is assumed that the biofilm density (X_f) in reactors to be uniform across the Z axis, as described by Rittmann and McCarty (2001). This simplification is necessary to evaluate the overall reaction between substrate utilization and biofilm. The substrate was transferred through liquid boundary layer (L_l) based on Fick's first law of diffusion. When substrate goes through the surface of biofilm to substratum, molecular diffusion is the major function for diffusing substrate into biofilm based on Fick's second law of diffusion (Rittmann and McCarty, 2001). Substrate concentration would decrease from the surface to substratum inside biofilm. The average thickness of biofilm in previous studies (Seibel and Characklis, 1991; Peyto and Characklis, 1993) were various from 6 to 40 μm under glucose loading rates between 10 to 120 mg/m^2. Because biofilm is very thin, the error caused by average substrate concentration ($\bar{S}_f$) is negligible.

Contact time in a biological reactor is a critical parameter to evaluate the degradation of substrate (Huang et al., 2011). In this study, HRT in the reactor was set at 30 min. Biofilm has a better capability to utilize BOM than suspended biomass (Gagnon, 1997). It was assumed that the degradation of amino acids was negligible in bulk water in this study. Therefore, the contact time and surface of biofilm could be combined into the steady-state amino acid flux (*J*) (Equation 5.1) (Gagnon and Huck, 2001). In this study, the different surface of materials (i.e., polypropylene rob and polycarbonate coupon) were regarded as having the same surface characteristic.

$$J = \frac{(S_i - S_b)}{\theta a} \qquad \text{Equation 5.1}$$

Where J is the BOM flux, mg/m^2.h;

S_i is substrate concentration of influent, mg/m^3;

S_b is substrate concentration of effluent, mg/m^3;

θ is hydraulic retention time, h;

a is specific surface area, m^{-1}.

Rittmann and McCarty (2001) described the diffusion of substrate inside the biofilm with Fick's second law of diffusion and Monod kinetics (Equation 5.2 to 5.3). According to mass balance, the flux of substrate in biofilm was equal to the substrate utilization rate (Equation 5.2).

$$D_f \frac{d^2 S_f}{dz^2} = \frac{k_{max} X_{f,v} S_f}{K_s + S_f} \qquad \text{Equation 5.2}$$

Where D_f is the molecular diffusivity in biofilm, m^2/s;

S_f is the biofilm substrate concentration, mg/m^3;

k_{max} is the maximum specific rate of substrate utilization, h^{-1};

$X_{f,v}$ is the bacterial density, mg/m^3;

K_s is the half- velocity constant, mg/m^3.

According the Equation 5.2, the flux on biofilm was equal to the utilization rate of amino acids integrated. Integrating from biofilm surface to coupon surface produces Equation 5.3.

$$\left[D_f \frac{dS_f}{dz}\right]_0^{L_f} = \int_0^{L_f} \frac{k_{max} X_{f,v} S_f}{K_s + S_f} \qquad \text{Equation 5.3}$$

It is impossible to use Equation 5.3 to integrate flux inside biofilm because S_f and $X_{f,v}$ are varied from surface of coupon ($Z = 0$) to the surface of biofilm ($Z = L_f$). Gagnon and Huck (2001) indicated that mass transfer would not limit BOM utilization. Therefore, the real biomass density and substrate concentration inside the biofilm can be represented as $\bar{X}_{f,v}$ and $\bar{S_f}$ which are the average values. Considering the biofilm and the liquid boundary layer were pretty thin, it can be regarded as the substrate concentration in bulk water was equal to the average substrate concentration in the biofilm. Equation 5.3 can be expressed as:

$$\bar{S_f} = S_b \qquad \text{Equation 5.4}$$

$$J = \frac{(S_i - S_b)}{\theta a} = \frac{k_{max} \bar{X}_{f,v} S_b L_f}{K_s + S_b} \qquad \text{Equation 5.5}$$

In this study, biomass ATP was applied to represent total biomass on coupons, which has been discussed in Chapter 4. Thus, $\bar{X}_{f,v}$ and L_f were replaced by the total ATP value ($tATP$) and the conversion factor between biomass ATP to biomass mass (k_{atp}) in Equation 5.6.

$$J = \frac{(S_i - S_b)}{\theta a} = \frac{k_{max}\ tATP\ k_{ATP}\ S_b}{K_s + S_b} \qquad \text{Equation 5.6}$$

5.3.2 Amino acid flux in biofilm reactors

Plotting the amino acid flux against the bulk amino acid solution concentration can determine the kinetic parameters for Equation 5.7 (shown in Figure 5.3).

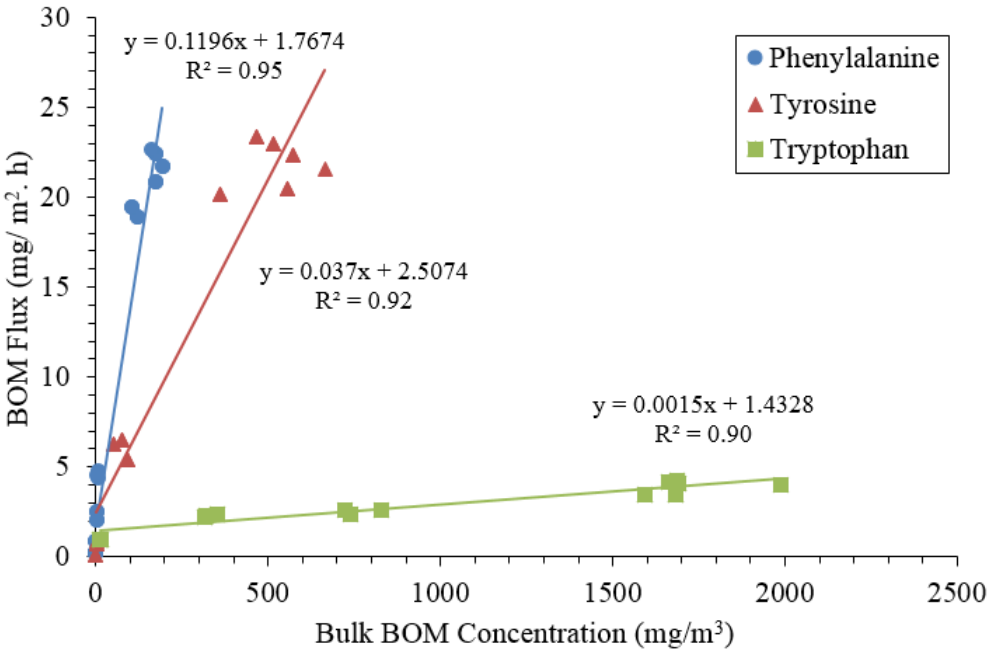

Figure 5.3 BOM flux versus bulk BOM concentration in CDC biofilm reactor.

In the biofilm reactor system, the observable kinetics can be expressed as the areal biodegradation rate k_a of BOM (Equation 5.7) (Gagnon and Huck, 2001). This first-order

relationship was observed by Huck et al. (1994) in full-scale biofilters and Gagnon and Huck (2001) in AR biofilm reactor.

$$J = \frac{(S_i - S_b)}{\theta a} = k_a S_b \qquad \text{Equation 5.7}$$

The k_a values (the slope in Figure 5.3) show that phenylalanine had the highest utilization rate among these amino acids evaluated in this study. Based on the model developed from Rittmann and McCarty (2001), a threshold concentration for growth (S_{min}) was defined as the minimum substrate concentration requirement for biofilm growth. In other words, if the substrate concentration was lower than S_{min}, biofilm cannot maintain its internal construction. Huck et al. (1994) suggested that the *x*-intercept (e.g., *x*-intercept in Figure 5.3) values represents the S_{min} for BOM removal in biofilters. Estimation of S_{min} for a pilot scale biofilter was found by other researchers to be in the range of 4.5 to 25 µg acetate C/L (Zhang and Huck, 1996). For synthetic water, an estimated S_{min} was determined to be 20.2 µg acetate C/L by Zhang and Huck, 1996. Gagnon and Huck (2001) observed a S_{min} (12µg C/L) in AR reactor using BOM cocktail consisted of aldehydes, carboxylic acids, and amino acids. In this study, the *x*-intercept values were negative. This suggests that bacterial affinity and biodegradation capability of amino acids are better than other NOMs and BOMs (e.g., carboxylic acid). Therefore, the biofilm growth and biofilm construction could be maintained at very low concentration of amino acids. In addition, free amino acids (aspartic acid, glutamatic acid, and serine) examined in Gagnon and Huck's study (2001) was near or close to the detection limit (0.1µg C/L) with influent concentrations of 7 to 670 µg C/L, which also indicated that the S_{min} of amino acids was very low.

van der Kooij et al. (1988; 1995) estimated that the threshold concentration endogenous metabolism of biofilm was 0.1µg C/L because biofilm formation could be at very low concentration of substrate. It is noted that the threshold concentration is related with incubation condition or biomass' structure (e.g., biofilm) because sloughing off processes would result in a higher threshold concentration (van der Kooij et al., 1995). Thus, S_{min} would be various in different reactors.

5.3.3 Relationship between biomass ATP and amino acid flux

Biomass ATP versus BOM flux in biofilm reactor is shown in Figure 5.4.

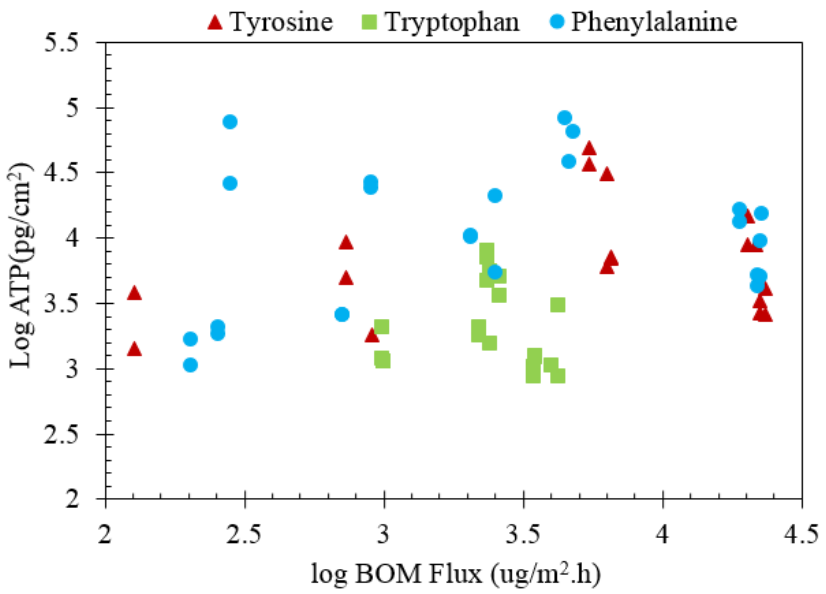

Figure 5.4 Biomass ATP versus BOM flux to the biofilm.

No linear relationship was found between biomass ATP and BOM flux. Therefore, the BOM flux was normalized to biomass ATP with bulk BOM concentration as shown in Figure 5.5 a-c.

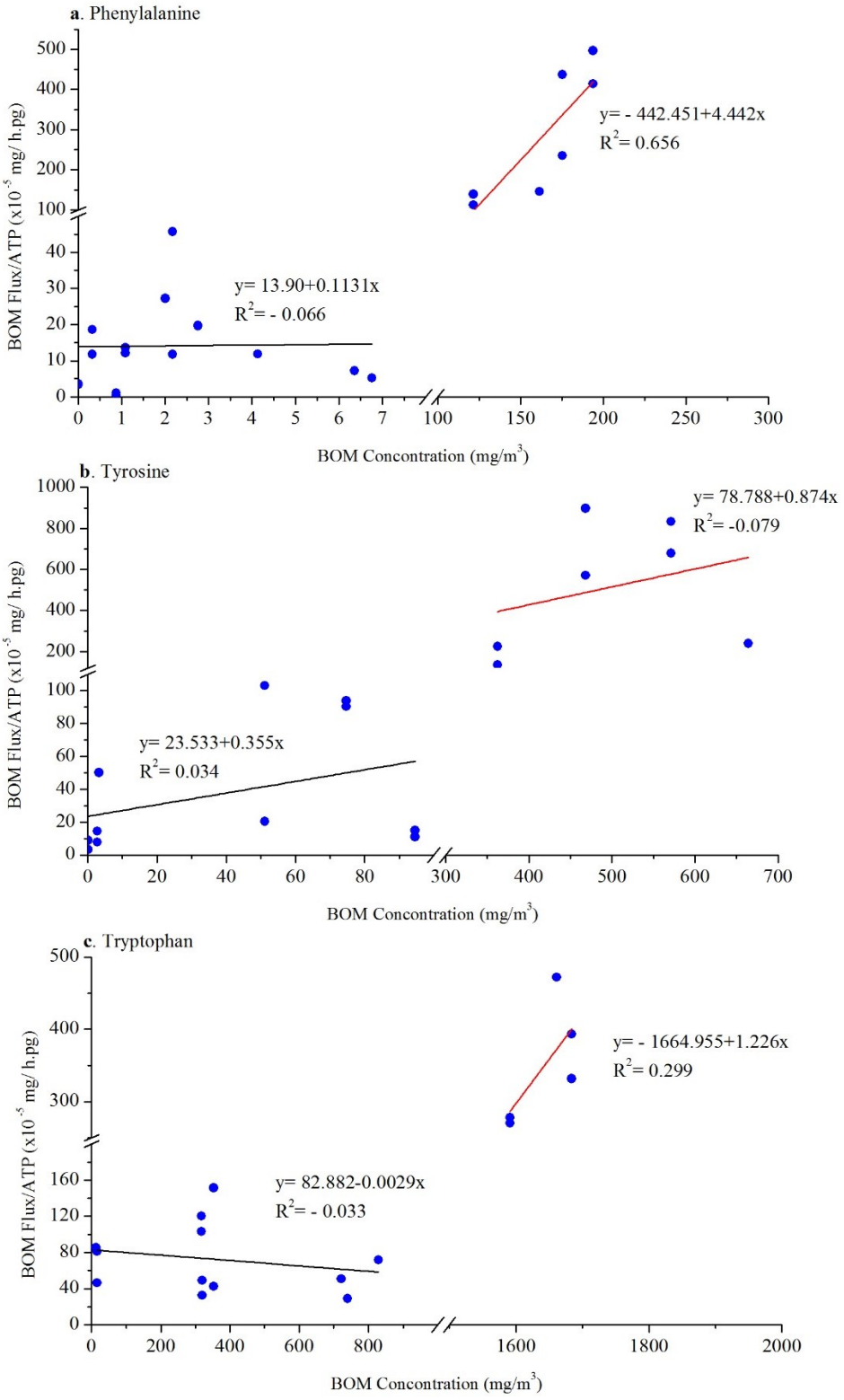

Figure 5.5 a-c Regression analysis of normalized BOM flux and the bulk BOM concentration.

In Figure 5.5 a-c, a linear regression was performed between BOM flux normalized to biomass ATP and the bulk BOM concentration (Equation 5.8). The slope of the line at low bulk BOM concentration was not significant and the R^2 was -0.066 to 0.034, indicating a general lack of fit. Therefore, the average estimated BOM flux/ATP at low and high bulk BOM concentration ranges calculated by Equation 5.8 are shown in Table 5.3. Gagnon and Huck (2001) reported the same relationship between BOM flux normalized to HPCs and the bulk BOM concentration.

$$\frac{J}{tATP} = \frac{J}{\bar{X}_{f,v}\, L_f} = \frac{k_{max} k_{ATP} S_b}{K_s + S_b} \qquad \text{Equation 5.8}$$

Table 5.3 Estimated BOM flux/ATP at low and high bulk concentration.

Water sample	Bulk BOM con. (mg/m^3)	Estimated BOM flux/ATP (10^{-5} mg/h.pg)
Tyrosine	0 to 100	≅ 38
	300 to 700	≅ 510
Tryptophan	0 to 100	≅ 73
	1500 to 1800	≅ 340
Phenylalanine	0 to 10	≅ 14
	100 to 200	≅ 280

The data presented in Table 5.3 shows that the phenylalanine test water had the lowest average estimated BOM flux/ATP at both low and high bulk BOM concentrations. This means phenylalanine had the highest conversion efficiency from substrate to biomass biological activity. The estimated BOM flux/ATP of tyrosine was higher than that of phenylalanine and tryptophan at high bulk concentration. In Chapter 4, biomass ATP in tyrosine-supplemented column was the lowest at target concentration of 3 mg/L

(3000mg/m^3), which suggested that the BOM flux/ATP of tyrosine would be lower than that of phenylalanine and tryptophan at high bulk BOM concentration.

For the estimated results presented in Figure 5.5 a-c and Table 5.3, no significant relationship was found with regression analysis. BOM flux/ATP can be regarded as an approximate constant at low bulk BOM concentration if $K_s \ll S_b$. In previous studies, Rittmann et al. (1986) reported the K_s value was about 5.27 acetate-C/L in an oligotrophic biofilm system. Average K_s of amino acid cocktail was about 8.0 μg C/L for *Aeromonas hydrophila* growth in drinking water (van der Kooij and Hijnen, 1988). These previous estimated K_s values are in good agreement with the experimental results in this study at low bulk concentration.

From the perspective of mass balance, ideally, BOM flux/ATP should be constant at both low and high bulk BOM concentrations if biomass ATP is linearly correlated with the mass ($\bar{X}_{f,v}\ L_f$)of biofilm. However, BOM flux/ATP at high bulk BOM concentration was higher than that at low BOM concentration. One possible reason for this is that biological activity decrease as biofilm thickness increase. At low concentration, thin biofilm can maintain very high active biomass about approach 100%, while some thick biofilms are dominated by inert biomass especially near the media surface (Rittman and McCarty, 2001). Therefore, for the biofilm at high bulk BOM concentration, the biological activity may be lower than thin biofilm at lower bulk BOM concertation. This also indicates that biomass ATP may be linearly correlated with removal percentage of BOM just in the certain range of BOM concentration.

Another possible reason is the hydraulic shear stress in biofilm reactor. At high concentration, the biofilm thickness would increase with higher BOM flux. During this process, the detachment rate of biofilm caused by hydraulic shear stress may reduce because the bacteria deep inside are protected from hydraulic shear stress. Rittmann (1982) suggested that b_{det} presents specific biofilm-detachment loss coefficient (T^{-1}) (Equation 5.9 and 5.10).

$$b_{det} = 8.42 \cdot \left[\frac{\sigma}{1 + 433.2\left(L_f - 0.003\right)}\right]^{0.58} \qquad \text{Equation 5.9}$$

For biofilm thickness L_f>0.003cm (3μm).

Where σ is the shear stress, g/(cm.s^2).

And

$$b_{det} = 8.42 \cdot \sigma^{0.58} \qquad \text{Equation 5.10}$$

For the biofilm thickness L_f<0.003cm (smooth surface)

Previous studies reported the steady-state biofilm thickness was in the range of 6μm to 40μm in biofilm reactor at glucose loading of 10 to 120 mg/m^2.h (Seibel and Characklis, 1991; Peyto and Characklis, 1993) and almost less 10μm in drinking water distribution system (Gagnon and Huck, 2001). In this study, the amino acid loading was in the range of about 0 to 25 mg/m^2.h. According to Equation 5.9 and Equation 5.10, the b_{det} would reduce if biofilm thickness on coupon was larger than 3μm as BOM flux (bulk BOM

concentration) increase. Because of the lower detachment rate, biofilm cannot keep a high biological activity for multiplication. Therefore, it is possible that the low detachment loss rate at high bulk BOM concentration may result in the lower biological activity measured by BOM flux/ATP value.

In addition, the microorganism community of coupon may have a great change after long-time feeding artificial amino acid solution because the biofilm was incubated from dechlorinated tap water (surface water). The changes in microorganism community may result in the reduced biological activity.

5.3 Conclusion

In this investigation of kinetics for amino acid supplementation, observed kinetics of degradation of amino acids can be modeled as a first-order model which has been proved in previous studies. Analysis of normalized BOM flux and bulk concentration showed that the conversion efficiency from BOM flux to biomass ATP would be a relative constant in certain bulk BOM concentration. With increased biomass thickness, hydraulic condition or the changes in microorganism community may result in the lower conversion efficiency at high BOM concentration.

Chapter 6 Conclusion

6.1 Conclusions

The batch experiment of filtered flocculated-water from J. D. Kline Water Supply Plant proved that amino acids can improve biomass ATP in water samples. The specific growth rates were improved by dosing amino acids while nitrogen supplement did not have the same effect on bacterial growth. After the exponential growth phase, there was no amino acid residual. This demonstrated that the bacteria in water samples have a great affinity to amino acids.

The bench-scale biofilter study indicated that amino acids can improve the biological activity of biofilm grown on filter media. Amino acid supplementation improved the average biomass ATP concentration up to 3.2×10^4 to 2.9×10^5 pg/cm^2. In addition, vertical variation of biomass ATP in biofitlers demonstrated that different types of amino acids will result in different amount of biomass ATP at the same target concentration of amino acids. The metabolic and catabolic pathways may have effects on the conversion efficiency between amino acids and biomass ATP.

As to degradation of amino acids, the first-order kinetic model was applied to determine the kinetics of the amino acid degradation (as measured by peCOD and DOC). peCOD was showed to be a better indicator than DOC for assessing the performance of biofilters. FEEMs of effluent indicated that there was no amino acid residual. Removal of NOMs may happen at very low NOM concentration in amino acid-supplemented columns.

The biofilm reactor study indicated that the first order model can be applied to the removal of amino acids with biofilm. The relationship between biofilm ATP concentration and bulk BOM concentration fits the kinetic models developed by Rittmann and McCarty (2001) and Gagnon and Huck (2001). At high BOM concentration, decreased detachment rate and the change of microorganism community may increase the values of BOM flux/ATP. This indicated the reduced the efficiency of energy conversion from amino acids to biomass ATP.

6.2 Recommendations

Further research on amino acid-supplemented biofilters in water treatment with amino acid supplementation should be performed in order to examine whether higher biological activity will result in a better removal of specific contaminants. It is noted that the operational conditions (e.g., continuous or discontinuous addition) and dosage of amino acids are important for the performance of enhanced biofilters.

The kinetics of amino acid degradation should be further investigated. The half velocity constant (K_s) of amino acids with biofilm should be determined by a more sophisticated experiment, because the range of K_s in previous studies was still controversial.

Even though FEEMs did not detect the residuals of phenylalanine, tyrosine, and tryptophan in the bench-scale biofilter study, the detection of products within the citric acid cycle and other catabolic pathways should be performed. This would be useful for understanding the procedure of amino acid degradation within microorganism in aqueous environments.

Biodiversity test (i.e., DNA sequencing analysis) should be performed, because the biodiversity of microorganisms can be affected by food sources.

References

Akashi, H., & Gojobori, T. (2002). Metabolic efficiency and amino acid composition in the proteomes of Escherichia coli and Bacillus subtilis. *Proceedings of the National Academy of Sciences*, *99*(6), 3695-3700.

Andersson, C. A., & Bro, R. (2000). The N-way toolbox for MATLAB. *Chemometrics and Intelligent Laboratory Systems*, *52*(1), 1-4.

Anraku, Y. (1978). Active transport of amino acids. *Bacterial transport* (pp. 171-219). New York: Marcel Dekker, Inc.

Baker, A. (2002). Fluorescence excitation-emission matrix characterization of river waters impacted by a tissue mill effluent. *Environmental Science & Technology*, *36*(7), 1377-1382.

Balconi, M. L., Borgarello, M., Ferraroli, R., & Realini, F. (1992). Chemical oxygen demand determination in well and river waters by flow-injection analysis using a microwave oven during the oxidation step. *Analytica chimica acta*, *261*(1-2), 295-299.

Baranyi, J. (2010). *Modelling and Parameter Estimation of Bacterial Growth with Distributed Lag Time*. University of Szeged, Hungary.

Baranyi, J., & Roberts, T. A. (1994). A dynamic approach to predicting bacterial growth in food. *International journal of food microbiology*, *23*(3-4), 277-294.

Barker, D. J., Mannucchi, G. A., Salvi, S. M., & Stuckey, D. C. (1999). Characterisation of soluble residual chemical oxygen demand (COD) in anaerobic wastewater treatment effluents. *Water Research*, *33*(11), 2499-2510.

Barker, H. A. (1981). Amino acid degradation by anaerobic bacteria. *Annual review of biochemistry*, *50*(1), 23-40.

Basu, O. D., Dhawan, S., & Black, K. (2015). Applications of biofiltration in drinking water treatment-a review. *Journal of Chemical Technology and Biotechnology, 91*(3), 585-595.

Bellar, T. A., Lichtenberg, J. J., & Kroner, R. C. (1974). The occurrence of organohalides in chlorinated drinking waters. *Journal (American Water Works Association)*, 703-706.

Boon, N., Pycke, B. F., Marzorati, M., & Hammes, F. (2011). Nutrient gradients in a granular activated carbon biofilter drives bacterial community organization and dynamics. *Water research*, *45*(19), 6355-6361.

Carstea, E. M., Baker, A., Bieroza, M., & Reynolds, D. (2010). Continuous fluorescence excitation-emission matrix monitoring of river organic matter. *Water research*, *44*(18), 5356

Chai, Y., Ding, H., Zhang, Z., Xian, Y., Pan, Z., & Jin, L. (2006). Study on photocatalytic oxidation for determination of the low chemical oxygen demand using a nano-TiO2-Ce (SO4) 2 coexisted system. *Talanta*, *68*(3), 610-615.

Chaiket, T., Singer, P. C., Miles, A., Moran, M., & Pallotta, C. (2002). Effectiveness of coagulation, ozonation, and biofiltration in controlling DBPs. *Journal-American Water Works Association*, *94*(12), 81-95.

Chen, J., LeBoeuf, E. J., Dai, S., & Gu, B. (2003). Fluorescence spectroscopic studies of natural organic matter fractions. *Chemosphenylalaninere*, *50*(5), 639-647.

Christensen, J. E., Dudley, E. G., Pederson, J. A., & Steele, J. L. (1999). Peptidases and amino acid catabolism in lactic acid bacteria. *Antonie van Leeuwenhoek*, *76*(1-4), 217-246.

ComBase (2015). DMFit web edition. https://browser.combase.cc/DMFit.aspx

Conley, W. R. (1972). High-rate Filtration. *Journal-American Water Works Association*, 203-206.

Delahaye, E., Welte, B., Levi, Y., Leblon, G., & Montiel, A. (2003). An ATP-based method for monitoring the microbiological drinking water quality in a distribution network. *Water Research*, *37*(15), 3689-3696.

Dotson, A., & Westerhoff, P. (2009). Occurrence and removal of amino acids during drinking water treatment. *Journal-American Water Works Association*, *101*(9), 101-115.

Dowdell, K. (2012). *Trace Organic Contaminant Removal in Drinking Water Biofilters under Carbonaceous and Nitrogen-Supplemented Conditions and Evaluating Biomass with ATP and Phospholipid Methods*. University of Colorado at Boulder, USA.

Evans, A. N. (2013). *The effect of nutrient limitations on the production of extracellular polymeric substances by drinking-water bacteria*. University of Texas at Austin, USA.
you

Findlay, R. H., King, G. M., & Watling, L. (1989). Efficacy of phospholipid analysis in determining microbial biomass in sediments. *Applied and Environmental Microbiology*, *55*(11), 2888-2893.

Gagnon, G. A. (1997). *Utilization of biodegradable organic matter by biofilms in drinking water distribution systems*. University of Waterloo, Canada.

Gagnon, G. A., & Huck, P. M. (2001). Removal of easily biodegradable organic compounds by drinking water biofilms: analysis of kinetics and mass transfer. *Water Research*, *35*(10), 2554-2564.

Granger, H. C., Stoddart, A. K., & Gagnon, G. A. (2014). Direct biofiltration for manganese removal from surface water. *Journal of Environmental Engineering*, *140*(4), 04014006-1-04014006-8.

Guilbault, G. G. (Ed.). (1990). *Practical fluorescence*. New York: Marcel Dekker Inc.

Halifax Water, (2014, March 31). *Eighteenth Annual Report*. Retrieved from http://www.halifax.ca/hrwc/documents/AnnualReportFinal-2014.pdf

Hammes, F. A., & Egli, T. (2005). New method for assimilable organic carbon determination using flow-cytometric enumeration and a natural microbial consortium as inoculum. *Environmental science & technology*, *39*(9), 3289-3294.

Hoffmann, M. R., Martin, S. T., Choi, W., & Bahnemann, D. W. (1995). Environmental applications of semiconductor photocatalysis. *Chemical reviews*, *95*(1), 69-96.

Huang, Z., Ong, S. L., & Ng, H. Y. (2011). Submerged anaerobic membrane bioreactor for low-strength wastewater treatment: effect of HRT and SRT on treatment performance and membrane fouling. *Water research*, *45*(2), 705-713.

Huck, P. M., & Gagnon, G. A. (2004). Understanding the distribution system as a bioreactor: a framework for managing heterotrophic plate count levels. *International journal of food microbiology*, *92*(3), 347-353.

Huck, P. M., Zhang, S., & Price, M. L. (1994). BOM removal during biological treatment: a first-order model. *Journal-the American Water Works Association*, *86*(6), 61-71.

Huisman, L., & Wood, W. E. (1974). *Slow sand filtration* (Vol. 16). Geneva: World Health Organization.

Kavan, L., Grätzel, M., Rathouský, J., & Zukalb, A. (1996). Nanocrystalline TiO2 (anatase) electrodes: surface morphology, adsorption, and electrochemical properties. *Journal of the electrochemical society*, *143*(2), 394-400.

Kim, Y. C., Sasaki, S., Yano, K., Ikebukuro, K., Hashimoto, K., & Karube, I. (2001). Photocatalytic sensor for the determination of chemical oxygen demand using flow injection analysis. *Analytica Chimica Acta*, *432*(1), 59-66.

Knowles, A. D., MacKay, J., & Gagnon, G. A. (2012). Pairing a pilot plant to a direct filtration water treatment plant. *Canadian Journal of Civil Engineering*, *39*(6), 689-700.

Lauderdale, C. V. (2011). *Engineered biofiltration for enhanced hydraulic and water treatment performance*. University of Florida, USA.

Lauderdale, C., Chadik, P., Kirisits, M. J., & Brown, J. (2012). Engineered biofiltration: Enhanced biofilter performance through nutrient and peroxide addition. *Journal-American Water Works Association, 104*(5) E298-E309.

LeChevallier, M. W., Schulz, W., & Lee, R. G. (1991). Bacterial nutrients in drinking water. *Applied and Environmental Microbiology*, *57*(3), 857-862.

LeChevallier, M. W., Shaw, N. E., Kaplan, L. A., & Bott, T. L. (1993). Development of a rapid assimilable organic carbon method for water. *Applied and Environmental Microbiology*, *59*(5), 1526-1531.

Li, C., & Song, G. (2009). Photocatalytic degradation of organic pollutants and detection of chemical oxygen demand by fluorescence methods. *Sensors and Actuators B: Chemical*, *137*(2), 432-436.

Li, L., Zhang, S., Li, G., & Zhao, H. (2012). Determination of chemical oxygen demand of nitrogenous organic compounds in wastewater using synergetic photoelectrocatalytic oxidation effect at TiO2 nanostructured electrode. *Analytica chimica acta*, *754*(2012), 47-53.

Li, X., Upadhyaya, G., Yuen, W., Brown, J., Morgenroth, E., & Raskin, L. (2010). Changes in the structure and function of microbial communities in drinking water treatment bioreactors upon addition of phosphorus. *Applied and environmental microbiology*, *76*(22), 7473-7481.

Liu, Y., Wang, A., & Claus, R. (1997). Molecular self-assembly of TiO2/polymer nanocomposite films. *The Journal of Physical Chemistry B*, *101*(8), 1385-1388.

Logsdon, G. S., Horsley, M. B., Freeman, S. D., Neemann, J. J., & Budd, G. C. (2006). Filtration processes-A distinguished history and a promising future. *Journal-American Water Works Association*, *98*(3), 150.

Magic-Knezev, A., & van der Kooij, D. (2004). Optimisation and significance of ATP analysis for measuring active biomass in granular activated carbon filters used in water treatment. *Water Research*, *38*(18), 3971-3979.

Metcalf & Eddy, Inc. (2003). *Wastewater Engineering: Treatment and Reuse*, New York: McGraw-Hill.

Miettinen, I. T., Vartiainen, T., & Martikainen, P. J. (1997). Phosphorus and bacterial growth in drinking water. *Applied and environmental microbiology*, *63*(8), 3242-3245.

Mihelcic, J. R., & Zimmerman, J. B. (2014). *Environmental engineering: Fundamentals, sustainability, design*. Wiley Global Education.

Miltner, R. J., Summers, R. S., & Wang, J. Z. (1995). Biofiltration performance: part 2, effect of backwashing. *Journal-the American Water Works Association*, *87*(12), 64-70.

Naidu, G., Jeong, S., Vigneswaran, S., & Rice, S. A. (2013). Microbial activity in biofilter used as a pretreatment for seawater desalination. *Desalination*, *309*(2013), 254-260.

Nerenberg, R., Rittmann, B. E., & Soucie, W. J. (2000). Ozone/biofiltration for removing MIB and geosmin. *Journal-American Water Works Association*, *92*(12), 85-95.

Peyton, B. M., & Characklis, W. G. (1993). A statistical analysis of the effect of substrate utilization and shear stress on the kinetics of biofilm detachment. *Biotechnology and Bioengineering*, *41*(7), 728-735.

Pharand, L., Van Dyke, M. I., Anderson, W. B., & Huck, P. M. (2014). Assessment of biomass in drinking water biofilters by adenosine triphosphate. *Journal-American Water Works Association*, *106*(10), E433-E444.

Pitter, P., & Chudoba, J. (1990). *Biodegradability of organic substance in the aquatic environment*. Boca Raton: CRC Press.

Ponnamperuma, C., Lemmon, R. M., Mariner, R., & Calvin, M. (1963). Formation of adenine by electron irradiation of methane, ammonia, and water. *Proceedings of the National Academy of Sciences*, *49*(5), 737-740.

Qiu, J., Zhang, S., & Zhao, H. (2012). Nanostructured TiO 2 photocatalysts for the determination of organic pollutants. *Journal of hazardous materials*, *211*, 381-388.

Rahman, I. (2013). *Direct biofiltration and nutrient (phosphorus) enhancement for polymeric ultrafiltration membrane fouling control*. University of Waterloo, Canada.

Rittman, B. E. (1982). The effect of shear stress on biofilm loss rate. *Biotechnology and Bioengineering*, *24*(2), 501-506.

Rittmann, B. & McCarty, P. (2001). *Environmental Biotechnology principles and applications*. Boston: McGraw-Hill.

Rittmann, B. E., Crawford, L., Tuck, C. K., & Namkung, E. (1986). In situ determination of kinetic parameters for biofilms: isolation and characterization of oligotrophic biofilms. *Biotechnology and bioengineering*, *28*(11), 1753-1760.

Sang, J., Zhang, X., Li, L., & Wang, Z. (2003). Improvement of organics removal by bio-ceramic filtration of raw water with addition of phosphorus. *Water research*, *37*(19), 4711-4718.

Sathasivan, A., & Ohgaki, S. (1999). Application of new bacterial regrowth potential method for water distribution system–a clear evidence of phosphorus limitation. *Water Research*, *33*(1), 137-144.

Servais, P., Billen, G., & Bouillot, P. (1994). Biological colonization of granular activated carbon filters in drinking-water treatment. *Journal of Environmental Engineering*, *120*(4), 888-899.

Shin, H. S., & Lim, K. H. (1996). Spectroscopic and elemental investigation of microbial decomposition of aquatic fulvic acid in biological process of drinking water treatment. *Biodegradation*, *7*(4), 287-295.

Siebel, M. A., & Characklis, W. G. (1991). Observations of binary population biofilms. *Biotechnology and bioengineering*, *37*(8), 778-789.

Sketchell, J., Peterson, H. G., & Christofi, N. (1995). Disinfection by-product formation after biologically assisted GAC treatment of water supplies with different bromide and DOC content. *Water research*, *29*(12), 2635-2642.

Srinivasan, R., & Sorial, G. A. (2011). Treatment of taste and odor causing compounds 2-methyl isoborneol and geosmin in drinking water: A critical review. *Journal of Environmental Sciences*, *23*(1), 1-13.

Stoddart, A. K., & Gagnon, G. A. (2014). Application of photoelectrochemical chemical oxygen demand to drinking water. *Journal- American Water Works Association*, *106*(9), E383-E390.

Stoddart, A.K., Schmidt, J.J., & Gagnon, G.A. (in press). Biomass evolution in full-scale anthracite-sand drinking water filters following conversion of biofiltration. *Journal-American Water Works Association.*

Teufel, R., Mascaraque, V., Ismail, W., Voss, M., Perera, J., Eisenreich, W., & Fuchs, G. (2010). Bacterial phenylalaninenylalanine and phenylalaninenylacetate catabolic pathway revealed. *Proceedings of the National Academy of Sciences*, *107*(32), 14390-14395.

Tifft, E. C., & Spiegel, S. J. (1976). Use of adenosine triphosphate assay in disinfection control. *Environmental science & technology*, *10*(13), 1268-1272.

Trueman, B. F., MacIsaac, S. A., Stoddart, A. K., & Gagnon, G. A. (2016). Prediction of disinfection by-product formation in drinking water via fluorescence spectroscopy. *Environmental Science: Water Research & Technology*, *2*(2), 383-389.

United States. Office of Drinking Water, & Smith, J. E. (1990). *Technologies for upgrading existing or designing new drinking water treatment facilities*. Office, US EPA.

Urfer, D., Huck, P. M., Booth, S. D., & Coffey, B. M. (1997). Biological filtration for BOM and particle removal: a critical review. *Journal-American Water Works Association*, *89*(12), 83-98.

Vadasarukkai, Y. S., & Gagnon, G. A. (2016). Characterization, fate and transport of floc aggregates in full-scale flocculation tanks. *Environmental Science: Water Research & Technology*, *2*(1), 223-232.

Vadasarukkai, Y. S., Gagnon, G. A., Campbell, D. R., & Clark, S. C. (2011). Assessment of hydraulic flocculation processes using CFD. *Journal-American Water Works Association.*, *103*(11), 66-80.

van der Kooij, D. (1992). Assimilable organic carbon as an indicator of bacterial regrowth. *Journal -American Water Works Association*, 57-65.

van der Kooij, D., & Hijnen, W. A. (1988). Nutritional versatility and growth kinetics of an *Aeromonas hydrophila* strain isolated from drinking water. *Applied and Environmental Microbiology*, *54*(11), 2842-2851.

van der Kooij, D., Veenendaal, H. R., Baars-Lorist, C., van der Klift, D. W., & Drost, Y. C. (1995). Biofilm formation on surfaces of glass and Teflon exposed to treated water. *Water research*, *29*(7), 1655-1662.

van der Kooij, D., Visser, A., & Hijnen, W. A. M. (1982). Determining the concentration of easily assimilable organic carbon in drinking water. *Journal-American Water Works Association*, 540-545.

Velten, S., Boller, M., Köster, O., Helbing, J., Weilenmann, H. U., & Hammes, F. (2011). Development of biomass in a drinking water granular active carbon (GAC) filter. *Water research*, *45*(19), 6347-6354.

Velten, S., Hammes, F., Boller, M., & Egli, T. (2007). Rapid and direct estimation of active biomass on granular activated carbon through adenosine tri-phosphate (ATP) determination. *Water Research*, *41*(9), 1973-1983.

Vodacek, A., Hogel, F. E., Swift, R. N., Yungel, J. K., Peltzer, E. T., & Blough, N. V. (1995). The use of in situ and airborne fluorescence measurements to determine UV absorption coefficients and DOC concentrations in surface waters. *Limnology and Oceanography*, *40*(2), 411-415.

Wang, J.Z., Summers, R.S., & Miltner, R.J. (1995). Biofiltration Performance: Part 1, Relationship to Biomass. *Journal-American Water Works Association*, *87* (12), 55-63.

Weishaar, J. L., Aiken, G. R., Bergamaschi, B. A., Fram, M. S., Fujii, R., & Mopper, K. (2003). Evaluation of specific ultraviolet absorbance as an indicator of the chemical composition and reactivity of dissolved organic carbon. *Environmental Science & Technology*, *37*(20), 4702-4708.

Yachi, S., & Loreau, M. (1999). Biodiversity and ecosystem productivity in a fluctuating environment: the insurance hypothesis. *Proceedings of the National Academy of Sciences*, *96*(4), 1463-1468.

Yu, J. C., Ho, W., Lin, J., Yip, H., & Wong, P. K. (2003). Photocatalytic activity, antibacterial effect, and photoinduced hydrophilicity of TiO2 films coated on a stainless steel substrate. *Environmental science & technology*, *37*(10), 2296-2301.

Zhang, S., & Huck, P. M. (1996). Parameter estimation for biofilm processes in biological water treatment. *Water Research*, *30*(2), 456-464.

Zhang, S., Zhao, H., Jiang, D., & John, R. (2004). Photoelectrochemical determination of chemical oxygen demand based on an exhaustive degradation model in a thin-layer cell. *Analytica Chimica Acta*, *514*(1), 89-97.

Zhao, W., Ma, W., Chen, C., Zhao, J., & Shuai, Z. (2004).

Yu, X., Zhang, X. J., Liu, X. L., Zhao, X. D., & Wang, Z. S. (2003). Phosphorus limitation in biofiltration for drinking water treatment. *Journal of Environmental Sciences*, *15*(4), 494-499.

Zearley, T. L., & Summers, R. S. (2012). Removal of trace organic micropollutants by drinking water biological filters. *Environmental science & technology*, *46*(17), 9412-9419. Efficient degradation of toxic organic pollutants with Ni2O3/TiO2-x B x under visible irradiation. *Journal of the American Chemical Society*, *126*(15), 4782-4783.

Zhu, L., Chen, Y. E., Wu, Y., Li, X., & Tang, H. (2006). A surface-fluorinated-TiO 2–KMnO 4 photocatalytic system for determination of chemical oxygen demand. *Analytica chimica acta*, *571*(2), 242-247.

Appendices

Appendix A-Chapter 3 Raw and Supplemental Data

Table A-1 TOC of filtered flocculated water

Sampling date (day)	0	1	2	3	4	5
Control #1 (mg TOC /L)	2.34	2.24	2.23	2.17	2.02	2.21
Control #2 (mg TOC /L)	2.22	2.23	2.21	2.23	2.12	2.11
NH4Cl #1 (mg TOC /L)	2.22	2.25	2.21	2.16	2.10	2.04
NH4Cl #2 (mg TOC /L)	2.30	2.24	2.18	2.22	2.17	2.10
Alanine #1 (mg TOC /L)	3.64	3.71	3.64	2.28	2.24	2.17
Alanine #2 (mg TOC /L)	3.86	3.86	3.59	2.30	2.24	2.18
Phenylalanine #1 (mg TOC /L)	4.14	4.11	3.48	2.41	2.64	2.53
Phenylalanine #2 (mg TOC /L)	4.19	4.21	3.48	2.41	2.53	2.38
Tryptophan #1 (mg TOC /L)	4.04	4.12	3.47	2.40	2.41	2.23
Tryptophan #2 (mg TOC /L)	4.07	4.01	2.69	2.40	2.28	2.37
Amino acid mixture #1 (mg TOC /L)	4.11	3.95	2.59	2.38	2.49	2.23
Amino acid mixture #2 (mg TOC /L)	4.10	4.00	2.64	2.42	2.53	2.24

Table A-2 ATP of filtered flocculated water

Sampling date (day)	0	1	2	3	4	5
Control (pg ATP/mL)	2.21	15.90	35.79	47.86	43.97	34.52
NH4Cl (pg ATP/mL	2.21	23.48	59.98	35.13	46.09	38.88
Alanine (pg ATP/mL)	2.21	24.77	293.24	1943.17	2475.84	1528.82
Phenylalanine (pg ATP/mL)	2.21	40.15	1886.40	4081.59	2627.10	2352.40
Tryptophan (pg ATP/mL)	2.21	31.70	1313.98	1640.49	1753.91	1427.80
Amino acid mixture (pg ATP/mL)	2.21	53.40	2731.50	2533.80	2258.14	2296.60

* The volume of sample for ATP test was 40 mL

Appendix B-Chapter 4 Raw and Supplemental Data

Table B-1 Biomass ATP of media with backwashing cycles

Sampling Date	Day	Phenylalanine (pg ATP/cm^2)	Tryptophan (pg ATP/cm^2)	Tyrosine (pg ATP/cm^2)	Control (pg ATP/cm^2)
2015/8/13	0	6204	15538	1923	973
2015/8/14	1	109269	164593	62186	2032
2015/8/15	2	132918	200216	75645	2472
2015/8/16	3	722416	583034	107666	6013
2015/8/17	4	753861	727229	55860	3383
2015/8/17	4	2179	2310	7684	320
2015/8/18	5	84298	19890	26473	1452
2015/8/19	6	325596	237515	56902	2025
2015/8/20	7	769466	294850	188864	3026
2015/8/21	8	918873	341276	202321	4928
2015/8/21	8	4893	1499	934	1189
2015/8/22	9	50184	13812	14809	701
2015/8/23	10	231646	116180	50416	1438
2015/8/24	11	512870	261555	91253	1774
2015/8/25	12	695463	411252	82439	2515
2015/8/25	12	7028	1158	1094	406

Table B-2 Estimated biomass ATP of filter media with estimated growth model

Tyrosine		Phenylalanine		Tryptophan		Control	
Time (hour)	Fit data (Ln ATP pg/cm^2)	Time (hour)	Fit data (Ln ATP pg/cm^2)	Time (hour)	Fit data (Ln ATP pg/cm^2)	Time (hour)	Fit data (Ln ATP pg/cm^2)
0	5.41	0	5.94	0	6.47	0	5.27
2.1	5.44	2.4	6	2.89	6.53	1.99	5.27
4.2	5.5	4.8	6.07	5.78	6.64	3.98	5.27
6.3	5.59	7.2	6.17	8.67	6.81	5.97	5.27
8.4	5.73	9.6	6.3	11.56	7.04	7.96	5.28
10.5	5.93	12	6.47	14.45	7.35	9.95	5.3
12.6	6.2	14.4	6.67	17.34	7.72	11.94	5.45
14.7	6.51	16.8	6.89	20.23	8.13	13.93	5.84
16.8	6.85	19.2	7.15	23.12	8.56	15.92	6.4
18.9	7.22	21.6	7.42	26.01	9.01	17.91	7
21	7.6	24	7.71	28.9	9.46	19.9	7.52
23.1	7.99	26.4	8	31.79	9.92	21.89	7.73
25.2	8.37	28.8	8.31	34.68	10.37	23.88	7.76
27.3	8.76	31.2	8.62	37.57	10.82	25.87	7.76

Tyrosine		Phenylalanine		Tryptophan		Control	
Time (hour)	Fit data (Ln ATP pg/cm^2)	Time (hour)	Fit data (Ln ATP pg/cm^2)	Time (hour)	Fit data (Ln ATP pg/cm^2)	Time (hour)	Fit data (Ln ATP pg/cm^2)
31.5	9.48	36	9.25	43.35	11.63	29.85	7.76
33.6	9.79	38.4	9.57	46.24	11.96	31.84	7.76
35.7	10.03	40.8	9.89	49.13	12.21	33.83	7.76
37.8	10.2	43.2	10.2	52.02	12.38	35.82	7.76
39.9	10.3	45.6	10.51	54.91	12.47	37.81	7.76
42	10.35	48	10.82	57.8	12.52	39.8	7.76
44.1	10.37	50.4	11.11	60.69	12.55	41.79	7.76
46.2	10.39	52.8	11.39	63.58	12.56	43.78	7.76
48.3	10.39	55.2	11.65	66.47	12.56	45.77	7.76
50.4	10.39	57.6	11.88	69.36	12.57	47.76	7.76
52.5	10.4	60	12.08	72.25	12.57	49.75	7.76
54.6	10.4	62.4	12.24	75.14	12.57	51.74	7.76
56.7	10.4	64.8	12.36	78.03	12.57	53.73	7.76
58.8	10.4	67.2	12.44	80.92	12.57	55.72	7.76
60.9	10.4	69.6	12.5	83.81	12.57	57.71	7.76
63	10.4	72	12.54	86.7	12.57	59.7	7.76
65.1	10.4	74.4	12.57	89.59	12.57	61.69	7.76
67.2	10.4	76.8	12.58	92.48	12.57	63.68	7.76
69.3	10.4	79.2	12.59	95.37	12.57	65.67	7.76
71.4	10.4	81.6	12.6	98.26	12.57	67.66	7.76
73.5	10.4	84	12.6	101.15	12.57	69.65	7.76
75.6	10.4	86.4	12.61	104.04	12.57	71.64	7.76
77.7	10.4	88.8	12.61	106.93	12.57	73.63	7.76
79.8	10.4	91.2	12.61	109.82	12.57	75.62	7.76
81.9	10.4	93.6	12.61	112.71	12.57	77.61	7.76
84	10.4	96	12.61	115.6	12.57	79.6	7.76
86.1	10.4	98.4	12.61	118.49	12.57	81.59	7.76
88.2	10.4	100.8	12.61	121.38	12.57	83.58	7.76
90.3	10.4	103.2	12.61	124.27	12.57	85.57	7.76
92.4	10.4	105.6	12.61	127.16	12.57	87.56	7.76
94.5	10.4	108	12.61	130.05	12.57	89.55	7.76
96.6	10.4	110.4	12.61	132.94	12.57	91.54	7.76
98.7	10.4	112.8	12.61	135.83	12.57	93.53	7.76
100.8	10.4	115.2	12.61	138.72	12.57	95.52	7.76
105	10.4	120	12.61	144.5	12.57	99.5	7.76

Table B-3 Data of tyrosine supplemented column

Time (hour)	DOC (mg/L)	PeCOD (mg/L)	DOC C/C_o	PeCOD C/C_o	FEEM Amino acids Fmax	FEEM NOM Fmax	FEEM Amino acids C/C_o	FEEM NOM C/Co	DOC Ln (C/Co)	peCOD Ln (C/Co)	ATP (pg/cm^2)
0	2.847	8.7	1.00	1.00	32.05	2.07	1.00	1.00	0.00	0.00	264
6	2.482	7.5	0.87	0.86	22.40	1.66	0.70	0.80	-0.14	-0.15	
8	-	-	-	-	-	-	-	-	-	-	221
12	2.029	6.3	0.71	0.72	7.44	1.69	0.23	0.82	-0.34	-0.32	507
17	1.757	5.5	0.62	0.63	2.90	1.89	0.09	0.91	-0.48	-0.46	1070
24	1.625	4.6	0.57	0.53	0.11	1.74	0.00	0.84	-0.56	-0.64	3139
30	1.64	3.9	0.58	0.45	0.14	1.66	0.00	0.80	-0.55	-0.80	11085
36	1.733	3.9	0.61	0.45	0.15	1.78	0.00	0.86	-0.50	-0.80	26088
42	1.728	3.1	0.61	0.36	0.10	1.78	0.00	0.86	-0.50	-1.03	14421
49	1.88	3.2	0.66	0.37	0.14	1.74	0.00	0.84	-0.41	-1.00	21775
52.5	-	-	-	-	-	-	-	-	-	-	19276
54	1.784	3.3	0.63	0.38	0.18	1.73	0.01	0.84	-0.47	-0.97	
56.5	-	-	-	-	-	-	-	-	-	-	27204
62	1.782	3.2	0.63	0.37	0.09	1.91	0.00	0.92	-0.47	-1.00	26371
73	2.007	3	0.70	0.34	0.11	2.09	0.00	1.01	-0.35	-1.06	42916
82	1.817	3.1	0.64	0.36	0.09	1.77	0.00	0.86	-0.45	-1.03	
84	-	-	-	-	-	-	-	-	-	-	49911
96	1.811	3.2	0.64	0.37	0.13	2.13	0.00	1.03	-0.45	-1.00	60594
105	-	-	-	-	32.05	2.07	-	-	-	-	62424

Table B-4 Data of tryptophan supplemented column

Time (hour)	DOC (mg/L)	PeCOD (mg/L)	DOC C/C_o	PeCOD C/C_o	FEEM Amino acids Fmax	FEEM NOM Fmax	FEEM Amino acids C/C_o	FEEM NOM C/Co	DOC Ln (C/Co)	peCOD Ln (C/Co)	ATP (pg/cm^2)
0	3.301	8.9	1.00	1.00	79.86	2.25	1.00	1.00	0.00	0.00	740
5	3.297	9.1	1.00	1.02	67.35	2.03	0.84	0.90	0.00	0.02	701
12	2.358	6.3	0.71	0.71	30.09	2.15	0.38	0.96	-0.34	-0.35	
14.5	-	-	-	-	-	-	-	-	-	-	1201
18	2.182	5	0.66	0.56	16.39	1.45	0.21	0.64	-0.41	-0.58	2682
25	1.86	5.3	0.56	0.60	0.17	1.47	0.00	0.65	-0.57	-0.52	
28	-	-	-	-	-	-	-	-	-	-	12810
30	1.787	4.9	0.54	0.55	0.13	1.39	0.00	0.62	-0.61	-0.60	
32.5	-	-	-	-	-	-	-	-	-	-	21663
36	1.851	4.7	0.56	0.53	0.25	2.21	0.00	0.98	-0.58	-0.64	
38	-	-	-	-	-	-	-	-	-	-	68107
42	1.899	4.7	0.58	0.53	0.23	2.34	0.00	1.04	-0.55	-0.64	
49	1.825	4.2	0.55	0.47	0.23	2.27	0.00	1.01	-0.59	-0.75	147134
54	1.901		0.58		0.19	2.42	0.00	1.08	-0.55		
56	-	-	-	-	-	-	-	-	-	-	202596
60	1.858	4.8	0.56	0.54	0.22	2.30	0.00	1.02	-0.57	-0.62	
62	-	-	-	-	-	-	-	-	-	-	173412
71	-	-	-	-	-	-	-	-	-	-	241951
72	1.901	4.6	0.58	0.52	0.40	2.34	0.01	1.04	-0.55	-0.66	
83	-	-	-	-	-	-	-	-	-	-	348159
84	1.851	4.2	0.56	0.47	0.37	2.39	0.00	1.06	-0.58	-0.75	-
96	1.799	4	0.54	0.45	-	-	-	-	-0.61	-0.80	-
99.5	-	-	-	-	-	-	-	-	-	-	466994
144.5	-	-	-	-	-	-	-	-	-	-	398923

Table B-5 Data of phenylalanine supplemented column

Time (hour)	DOC (mg/L)	PeCOD (mg/L)	DOC C/C_o	PeCOD C/C_o	DOC Ln (C/Co)	peCOD Ln (C/Co)	ATP (pg/cm^2)
0	3.187	9.5	1	1	0	0	445
6	3.189	9.9	1.00	1.04	0	-0.04	-
8	-	-	-	-	-	-	527
12	2.921	8.5	0.92	0.89	-0.09	-0.14	525
17	2.869	7.1	0.90	0.75	-0.11	-0.23	864
24	2.247	5.8	0.70	0.61	-0.35	-0.44	2109
30	1.921	4.8	0.60	0.51	-0.51	-0.52527	4600
36	1.684	4	0.53	0.42	-0.64	-0.7714	10968
42	1.625	2.5	0.51	0.26	-0.67	-	40097
49	1.725	3.5	0.54	0.37	-0.61	-0.92168	58193
54	1.786	3.1	0.56	0.33	-0.58	-1.00624	-
56.5	-	-	-	-	-	-	107334
60	1.713	3.2	0.54	0.34	-0.62	-1.09861	
62	-	-	-	-	-	-	134342
73	1.765	3.2	0.55	0.34	-0.59	-0.89501	240072
82	1.841	3	0.58	0.32	-0.55	-1.1653	-
84	-	-	-	-	-	-	157018
96	1.9	3	0.60	0.32	-0.52	-1.09861	506961
105	-	-	-	-	-	-	455275
120	-	-	-	-	-	-	319716

90

Table B-6 Data of control column

Time (hour)	DOC (mg/L)	PeCOD (mg/L)	DOC C/C_o	PeCOD C/C_o	FEEM NOM1 Fmax	FEEM NOM2 Fmax	FEEM Amino acids C/C_o	FEEM NOM C/Co	DOC Ln (C/Co)	peCOD Ln (C/Co)	ATP (pg/cm^2)
0	1.774	4.6	1.00	1.00	0.58	1.41	1.00	1.00	0.00	0.00	249
5	1.708	5.4	0.96	1.17	0.57	1.34	0.99	0.95	-0.04	0.00	151
12	1.716	5	0.97	1.09	0.56	1.42	0.96	1.00	-0.03	-0.06	
14.5	-	-	-	-	-	-	-	-	-	-	400
18	1.768	4.4	1.00	0.96	0.57	1.39	0.99	0.98	0.00	-0.13	1135
25	1.758	4.4	0.99	0.96	-	-	-	-	-0.01	0.00	
28	-	-	-	-	-	-	-	-	-	-	2293
30	1.748	4	0.99	0.87	0.58	1.38	1.00	0.97	-0.01	-0.24	
32.5	-	-	-	-	-	-	-	-	-	-	2132
36	1.788	4.5	1.01	0.98	0.85	2.66	1.00	1.00	0.01	-0.24	
38	-	-	-	-	-	-	-	-	-	-	2127
42	1.775	4	1.00	0.87	-	-	-	-	0.00	-0.29	
49	1.775	4	1.00	0.87	0.85	2.65	1.00	1.00	0.00	-0.32	2552
54	1.84	-	1.04	-	0.93	2.52	1.09	0.95	0.04	-	
56	-	-	-	-	-	-	-	-	-	-	2489
60	1.76	4.4	0.99	0.96	-	-	-	-	-0.01	-0.22	
62	-	-	-	-	-	-	-	-	-	-	2217
71	-	-	-	-	-	-	-	-	-	-	3153
72	1.815	4.3	1.02	0.93	0.90	2.27	1.06	0.85	0.02	-0.19	
83	-	-	-	-	-	-	-	-	-	-	2038
84	1.772	3.7	1.00	0.80	0.85	2.95	1.00	1.11	0.00	-0.35	-
96	1.745	3.6	0.98	0.78	-	-	-	-	-0.02	-0.32	-
99.5	-	-	-	-	-	-	-	-	-	-	2260

91

Appendix C-Chapter 5 Raw and Supplemental Data

Table C-1 Date of biofilm reactor

Tyrosine			Tryptophan			Phenylalanine		
Influent (μg/L)	Effluent (μg/L)	ATP (pg/cm^2)	Influent (μg/L)	Effluent (μg/L)	ATP (pg/cm^2)	Influent (μg/L)	Effluent (μg/L)	ATP (pg/cm^2)
421.80	51.13	6115.79	872.94	721.24	5067.69	286.98	6.36	66508.73
421.80	51.13	31065.75	877.86	739.82	8077.58	267.59	6.76	84397.62
414.97	94.58	36622.82	981.90	829.13	3623.02	273.97	4.13	38743.03
414.97	94.58	49323.20	494.14	353.03	1585.08	149.59	2.17	21250.70
458.85	74.70	7236.71	494.14	353.03	5661.88	149.59	2.17	5480.36
458.85	74.70	6965.24	446.05	317.68	1815.07	122.46	2.76	10308.19
45.76	2.71	9402.21	446.05	317.68	2118.29	122.46	2.76	10430.02
45.76	2.71	5035.26	456.98	319.79	7129.85	52.78	-	26712.17
7.59	0.12	1428.46	456.98	319.79	4753.23	52.78	-	24565.16
7.59	0.12	3796.87	61.20	14.43	335.53	12.18	0.33	1080.77
56.43	3.24	1804.37	61.20	14.43	390.66	12.18	0.33	1710.62
1842.00	468.00	4095.60	73.34	15.50	2116.07	16.02	1.09	1854.50
1842.00	468.00	2605.61	73.34	15.50	1213.10	16.02	1.09	2104.07
1863.62	514.87	-	71.66	13.26	1162.66	17.30	0.88	77526.26
1863.62	514.87	-	71.66	13.26	1162.66	17.30	0.88	26380.84
1883.10	571.38	2679.16	1907.00	1661.00	3055.96	43.35	2.00	2581.61
1883.10	571.38	3284.65	1907.00	1661.00	886.70	43.35	2.00	2581.61
1547.01	362.31	8948.05	1936.64	1687.14	-	1470.00	194.00	5251.21
1547.01	362.31	14920.90	1936.64	1687.14	-	1470.00	194.00	4372.51
1757.71	557.01	-	1885.99	1683.86	1037.53	1401.78	175.34	-
1757.71	557.01	-	1885.99	1683.86	874.35	1401.78	175.34	-
1929.93	664.09	9018.92	1794.75	1591.05	1282.46	1491.60	175.35	9519.65
-	-	-	1794.75	1591.05	1247.93	1491.60	175.35	5126.87
-	-	-	1930.84	1692.51	-	1233.90	121.42	13591.18
-	-	-	1930.84	1692.51	-	1233.90	121.42	16865.71
-	-	-	2223.71	1989.20	1070.97	1246.41	102.99	-
-	-	-	-	-	-	1246.41	102.99	-
-	-	-	-	-	-	1490.65	161.55	15507.88